INVESTIGATION ON THE PERFORMANCE OF BIOSORBENT AND ACTIVATED CARBON IN THE REMOVAL OF CATIONIC CONTAMINANT FROM WATER

KAYSHNI A/P LINGESWARAN

A project report submitted in partial fulfilment of the requirements for the award of Bachelor of Engineering (Honours) Chemical Engineering

Lee Kong Chian Faculty of Engineering and Science
Universiti Tunku Abdul Rahman

April 2020

DECLARATION

I hereby declare that this project report is based on my original work except for citations and quotations which have been duly acknowledged. I also declare that it has not been previously and concurrently submitted for any other degree or award at UTAR or other institutions.

Signature : _____

Name : Kayshni A/P Lingeswaran

ID No. : 1601445

Date : 18 May 2020

APPROVAL FOR SUBMISSION

I certify that this project report entitled **"INVESTIGATION ON THE PERFORMANCE OF BIOSORBENT AND ACTIVATED CARBON IN THE REMOVAL OF CATIONIC CONTAMINANT FROM WATER"** was prepared by **KAYSHNI A/P LINGESWARAN** has met the required standard for submission in partial fulfilment of the requirements for the award of Bachelor of Engineering (Honours) Chemical Engineering at Universiti Tunku Abdul Rahman.

Approved by,

Signature   :

Supervisor   :   Dr. Ng Yee Sern

Date   :   18 May 2020

ACKNOWLEDGEMENTS

I would like to express my sincerest gratitude to my supervisor, Dr. Ng Yee Sern, for his invaluable guidance and supervision throughout this project. I could not have completed this project without his attentiveness towards the progress of my project and the prompt responses I received to my questions and queries.

I am also very grateful for the laboratory staff and my course mates for their willingness to lend a helping hand to me so I could complete my experiments successfully. I am also very thankful for the emotional support and encouragement my family and friends has shown me for the entire duration of this research.

Lastly, a huge thank you to all the researchers from past studies that have contributed to this field of study as they have provided me with a better understanding of the subject matter.

ABSTRACT

Nickel ions which are commonly found in the wastewater discharge of a variety of industries pose serious threats to ecosystems and human health if their concentrations exceed permissible limits. Activated carbon adsorption is typically employed in the treatment of wastewater to remove heavy metal contaminants such as nickel from water. However, the cost of activated carbon itself is high. Longan peel was proposed as a low-cost biosorbent substitute to activated carbon. The present study focuses on investigating and comparing the efficiency of both these adsorbents in removing nickel (II) ions from aqueous solutions. Operating parameters which are initial nickel concentration, adsorbent dosage, and pH were examined to analyse the effects that they have on the removal of nickel ions. Based on Box-Behnken design of experiments, reduced cubic models were proposed to correlate the three independent variables for maximum removal efficiencies at optimum conditions. The maximum removal efficiency of nickel (II) by longan peel biosorbent was determined to be 47.64 % at optimal parameters: initial nickel concentration of 180.17 mg/L, biosorbent dosage of 9.708g, and pH 5.346. Optimal conditions for activated carbon were found to be initial nickel concentration of 11.94 mg/L, biosorbent dosage of 7.585 g, and pH 7.999, which resulted in a maximum removal efficiency of 97.85 %. Langmuir isotherm and Freundlich isotherm models exhibited the best fits for the equilibrium data for longan peel and activated carbon respectively. Despite the potential that longan peel biosorbent has shown in removing nickel ions from contaminated water, its performance pales in comparison to activated carbon and other low-cost biosorbents. Several suggestions were made to help overcome the shortcomings that the longan peel biosorbent has in terms of its adsorption capacity. In addition, recommendations for future research related to increasing the feasibility of adopting longan peel biosorbent in actual wastewater treatment plants were also presented.

TABLE OF CONTENTS

LIST OF TABLES

LIST OF FIGURES

LIST OF SYMBOLS / ABBREVIATIONS

C_e	equilibrium concentration of the adsorbate in the solution, mg/L
C_f	final concentration of adsorbate in the solution, mg/L
C_o	initial concentration of adsorbate in the solution, mg/L
K_L	constant that relates to the free energy of adsorption
K_F	constant that correlates to the relative adsorbent adsorption
m	dosage of the adsorbent, g or g/L
n	measure of the adsorption intensity of the adsorbate
q_e	adsorption capacity at equilibrium state, mg/g
q_m	maximum adsorption capacity of the monolayer, mg/g
q_t	adsorption capacity at a time of t, mg/g
R^2	coefficient of determination
R_L	separation factor
T	temperature, ^{o}C
V	volume of the solution, L

α	level of significance

ANOVA	Analysis of variance
AC	Activated carbon
BDL	Below detection limit
df	Degree of freedoms
FTIR	Fourier-transform infrared spectroscopy
ICP-OES	Inductively coupled plasma-optical emission spectrometry
RSM	Response surface methodology

CHAPTER 1

INTRODUCTION

1.1   General Introduction

The pollution of water is the consequence of the presence of physical, chemical, or biological components that diminish the condition of water bodies. Contaminated water may be regarded as unfit for drinking by humans, but still serve other roles such as the habitat of aquatic organisms, irrigation of crops, or be used for recreational purposes. Although natural events are known to cause water pollution, anthropogenic sources of pollution are the focus of many research topics (Schweitzer and Noblet, 2017).

Heavy metal contaminants in water occur naturally but they can become enriched through their extraction or use in industries to the point that they compromise water quality or stop adhering to safe drinking water regulations. Based on the analysis of industrial effluents, the most common heavy metal pollutants are nickel, lead, copper, mercury, zinc, cadmium, and chromium (Bahadir et al., 2007). Besides being highly toxic for living organisms, they accumulate in the food chain and persist in nature which makes them significant threats to both the environment and the welfare of the public.

Heavy metals are an integral part of many industries such as mining, smelters, surface finishing, textile, electroplating, aerospace, and various others where they are used extensively as compounds and as alloys in numerous applications. However, problems arise when these industries discharge substantial amounts of wastewater into the surface water and groundwater. As a result of the release of wastewater containing raw materials, the heavy metals disperse into water bodies and cause highly critical environmental problems through disruption of the ecosystem (Gürel, 2017).

Based on these reasons, removing and recovering the heavy metals contained within the wastewater is crucial from an economic and environmental standpoint. As such, several treatment techniques were developed in the past few years to facilitate the reduction of the quantity of these unwanted pollutants from aqueous solutions. These techniques are split into three categories which are chemical, physical, and biological. Among the removal techniques, chemical precipitation, electrochemical

process, ion exchange, membrane filtration, coagulation with flocculation, and adsorption have risen in prominence as they have shown promising results and potential of being implemented in real-scale applications. By evaluating each of the methods, it is apparent that they all have their own set of advantages and drawbacks.

Among these methods, the use of activated carbon for adsorption has gained a reputation of being highly efficient and effective as well as displaying an ability to simultaneously remove both metal and organic contaminants. However, it also exhibits disadvantages such as the high treatment cost of pollutants that are adsorbed by the activated carbon after the adsorption process (Wang, Lu and Li, 2016). Besides that, the treatment of large volumes of wastewater produced through adsorption incurs excessive expenditures. Consequently, there has been an influx in the interest of finding an economically-feasible, environmentally-safe, and effective substitute to activated carbon. Through the investigation of many researchers, waste biomass has demonstrated superior properties of adsorption when compared to using industrial or mineral waste (Ahmaruzzaman, 2011).

1.2   Importance of the Study

The present study evaluates the viability of longan peels as a biosorbent in removing excessive amounts of nickel ions contained in wastewater. The performance of longan peels in the batch adsorption tests will help in determining the potential of longan peels biosorbent when compared to activated carbon which has already established itself to be an adsorbent effective at adsorbing nickel ions. The results may serve as a starting point for research to be organised in the future to find a way to implement longan peels as a biosorbent for large scale treatment of nickel removal. If successful, this technique will give tremendous prospects in developing countries where the resources are scarce and where utilisation of lower-cost removal techniques can help lessen the financial impacts of wastewater treatment. Furthermore, the use of waste biomass such as the peels of fruits is an excellent way to help alleviate the ongoing waste management crisis.

1.3   Problem Statement

Nickel ions are commonly found in the wastewater discharge of various types of industries and have proven to be toxic at even low concentrations for humans to

drink as well as being a detrimental habitat for the living organisms present in the aqueous environment.

Standard A for the wastewater discharges that are upstream of raw water intake is 0.20 mg/L whereas Standard B for discharges that are downstream of raw water intake is 1.0 mg/L. These standards are set by Environmental Quality (Industrial Effluents) Regulations 2009 to determine the permissible nickel concentrations in wastewater effluent of industries (Department of Environment, 2010). The repercussions for parties found guilty of violating this regulation as enforced by Environmental Quality Act 1974 include a fine that does not exceed a sum of RM 100,000 or sentencing to a prison term that does not exceed five years or to both and to a fine that does not exceed RM 100,000 a day for each day that the contravention is continued after being served the notice by the Director General that requires the party to halt the act (Department of Environment, 2009).

Conventional methods used in wastewater treatment plants to reduce levels of nickel each have their setbacks. Activated carbon adsorption has emerged as a very efficient technique owing to its high efficiency and simplicity of process design (Papageorgiou et al., 2009). However, its applicability is hindered by the high cost of the activated carbon itself.

In light of this, there is a need to develop an economical and commercially viable method for the removal of nickel in wastewater while also taking into consideration its performance, cost, design, and operation.

1.4   Aim and Objectives

The ultimate purpose of the current research is to review the practicality of using longan peels as a biosorbent in removing nickel ion contaminants from aqueous solutions. The present study aims to accomplish the following objectives:

(i)   To investigate the removal efficiency and adsorption uptake of nickel ions using longan peel biosorbent.

(ii)   To investigate the effects of initial concentration, adsorbent dosage, and pH on the adsorption performance of the longan peels.

(iii) To compare the performance of longan peel biosorbent and commercial activated carbon in the removal of nickel from water.

1.5 Scope of the Study

The present study encompasses the procedure for carrying out the batch adsorption studies, characterisation of longan peel biosorbent and activated carbon, analysis of the experimental data based on the design of experiments by response surface methodology (RSM), and optimisation to maximise the removal efficiencies. Nickel ions were chosen for the study as it is one of the most prevalent heavy metal contaminants that are present in the wastewater discharge of various industries. Longan peels were selected as the biosorbent as they are readily available, cheap, and under-researched in this field of study. The parameters that affect adsorption performance which are initial concentration, pH, and adsorbent dosage were chosen to be investigated.

1.6 Outline of the Report

The study covers four main chapters:

(i) Chapter 1 introduces the background, importance, aim, problem statements, and the overall scope of the study.

(ii) Chapter 2 covers the literature review of journal articles, books, and web resources on the topics related to this study. Its subtopics include the introduction to nickel ion and the purpose of its removal from wastewater, the conventional methods of cationic removal, description of the adsorption and biosorption processes, biosorbents studied in previous research, as well as the theories underlying adsorption isotherm and response surface methodology (RSM).

(iii) Chapter 3 outlines the materials, chemicals, and equipment involved to carry out the experiments, the process flow of the experiments, the parameters to be investigated in the batch adsorption studies, the generation of the design matrix for response surface methodology, the descriptions of the analytical method as well as the method to investigate the best-fitting adsorption isotherm.

(iv) Chapter 4 involves the analysis of FTIR spectra of both adsorbents, models fitting, the interpretation of ANOVA of the models, study of the effects of the individual parameter and their combined effects via RSM, optimisation of parameters for maximum removal efficiency,

and determining the feasibility of longan peel biosorbents in wastewater treatment plants.

(v)   Chapter 5 highlights the significant findings in the study, the conclusion of the results, and several proposed recommendations to improve future research in this area of study.

CHAPTER 2

LITERATURE REVIEW

2.1   General Introduction to Nickel Ion

Nickel is the 28th element of the periodic table where it is a member of the iron group of transitional metals and can exist as oxidation states from +1 to +4. Under typical environmental conditions, nickel typically exists in the oxidation state of Ni(II), whereby nickel is in the +2 valence state (Cempel and Nikel, 2006). When in neutral water, nickel (II) ions are present as the greenish hexahydrated $[Ni(H_2O)_6]^{2+}$ ions (Savolainen, 1996). Nickel exhibits corrosion-resistant properties towards alkali, water, and air, but is extremely soluble in dilute oxidising acids. The physical properties of nickel are tabulated in Table 2.1.

Table 2.1: Physical Properties of Nickel (Royal Society of Chemistry, 2019)

Physical Property	Value
Atomic number	28
Relative atomic mass	58.693
Density (g/cm^3)	8.90
Boiling point (^{o}C)	2913
Melting point (^{o}C)	1455

Some of the applications of nickel in the industry are in nickel electroplating, battery manufacturing, copper sulfate production, leather tanning, dyeing operation, paint formulation, ceramic and porcelain enamelling, and steam-electric power plants (Gupta, Rastogi and Nayak, 2010). The nickel concentrations of the industrial effluents differ vastly from one industry to another as depicted in Table 2.2.

Table 2.2: Concentration of Nickel (II) Ion in Wastewater of Various Industries

Source	Industry	Nickel Concentration (mg/L)	Reference
Ambattur Industrial Estate, Chennai, India	Electroplating	132.0	(Sivakumar et al., 2018)
Sigma Electroplating Industry, India	Electroplating	5.820	(Husain et al., 2014)
Unspecified metal finishing factory, Yalova, Turkey	Metal plating	248.0 - 282.0	(Kabdaşli et al., 2009)
Unspecified nickel plating plant in Taiwan	Nickel plating plant	2900	(Shih, Lin and Huang, 2013)
Selected companies in Lagos, Nigeria	Paint manufacturing	BDL -1.900	(Aniyikaiye et al., 2019)
Survey by U.S. Environmental Protection Agency	Battery manufacturing	2.493	(Ruckelshaus, Ravan and Johnson, 1984)
Houjing Plating Industry Park, Zhejiang Province	Electroplating	238.0 - 300.0	(Porex Corporation, 2013)
Unspecified electroplating factory in Thailand	Electroplating	96.10	(Srisuwan and Thongchai, 2002)
Industrial effluents from Haryana and Chandigarh	Electroplating	72.00 - 243.0	(Singh and Ram, 2016)
Four unspecified electroplating sites from Agra city	Electroplating	5.640 - 27.00	(Singh and Verghese, 2006)
Unspecified gold mine in Finnish Lapland	Gold mining	0.03700 - 0.06800	(Palmer, Ronkanen and Kløve, 2015)

2.2 Purpose of Nickel Ion Removal in Wastewater

Besides being non-biodegradable, nickel is known to exhibit hazardous effects on human beings and other living organisms at even minuscule amounts. The ability of nickel to undergo redox cycling between Ni^{2+} and Ni^{3+} is one of the attributes that contribute to its toxicity (Savolainen, 1996).

One of the major routes of human exposure to nickel is absorption via direct skin contact where it has the potential to cause skin dermatitis. Previous reports suggest that certain nickel compounds like nickel carbonyl are also rapidly absorbed into the skin and discovered to be lethal to humans at exposure levels of 30 ppm for 30 minutes (Vieira et al., 2010). Furthermore, serious health impacts such as gastrointestinal discomfort, lung and kidney damage, renal edema, and pulmonary fibrosis are caused by prolonged exposure to excessive doses of nickel (Pahlavanzadeh et al., 2010). Apart from that, past studies have reported on the ability of nickel to traverse the human placental barrier and reach the foetus, whereby it can cause tetragenesis or embryotoxicity (Chen and Lin, 1998).

The International Agency for Research on Cancer (IARC) in 1990 determined that compounds of nickel belong to Group 1 which is the carcinogenic category while metallic nickel is placed in Group 2B as possibly carcinogenic to humans. However, there is a lack of evidence of the correlation between oral exposure to nickel and carcinogenic risk (World Health Organization, 2005).

Environmental Quality (Industrial Effluents) Regulations 2009 set nickel concentrations of 0.20 mg/L as Standard A for the discharges of wastewater that are upstream of the intake of raw water and 1.0 mg/L as Standard B for the discharges that are downstream of the intake of raw water (Department of Environment, 2010). Besides, the National Water Quality Standards for Malaysia has taken the various health impacts caused by nickel into account and established the maximum permissible concentration of nickel according to their uses as shown in Table 2.3. Consequently, it is extremely important to carry out the treatment of industrial effluents contaminated by excessive amounts of nickel ions before they are discharged into the environment.

Table 2.3: Maximum Allowable Limit of Nickel Concentrations in Water Bodies
(Water Environment Partnership in Asia, 2006)

Water Class	Uses	Maximum Permissible Limit of Nickel (mg/L)
I	Natural environment conservation. Water supply without any necessary treatment. Fishery consisting of highly sensitive aquatic organisms.	Completely absent or present at natural levels
IIA	Water supply treated conventionally. Fishery consisting of sensitive aquatic organisms.	0.05
IIB	Recreational use where contact with the body may occur.	0.05
III	Water supply with the need for large scale treatment required. Fishery consisting of common commercial value and tolerant aquatic organisms. Source of water for livestock.	0.90
IV	Irrigation	0.20

2.3 Conventional Methods of Cationic Removal

Over the years, the research and development field specialising in wastewater treatment has seen an influx of studies to effectively remove heavy metal contaminants from wastewater. As a result, many new methods such as membrane filtration, chemical precipitation, electrochemical process, coagulation-flocculation, and ion exchange have emerged and been the subject of continuous investigation.

2.3.1 Membrane Filtration

By employing the use of a membrane, a concentration or pressure gradient acts as the driving force to facilitate the mechanical and chemical screening of undesired macromolecules and particles in the wastewater (Benjamin and Lawler, 2013).

2.3.1.1   Process Description

Membrane filtration is a gentle, physical separation operation where the emulsion of contaminants is neither thermally nor chemically altered. Based on the criteria for separation of compounds such as particle size and polarity, the membranes have the capacity to hold specific substances back while the others selectively pass through the membrane. The driving forces that enable the mass flow of the particles through the membrane are the gradients of pressure or concentration between both sides of the membrane (Graff, 2012). A typical scheme showing the utilisation of membrane filtration in wastewater treatment is depicted in Figure 2.1.
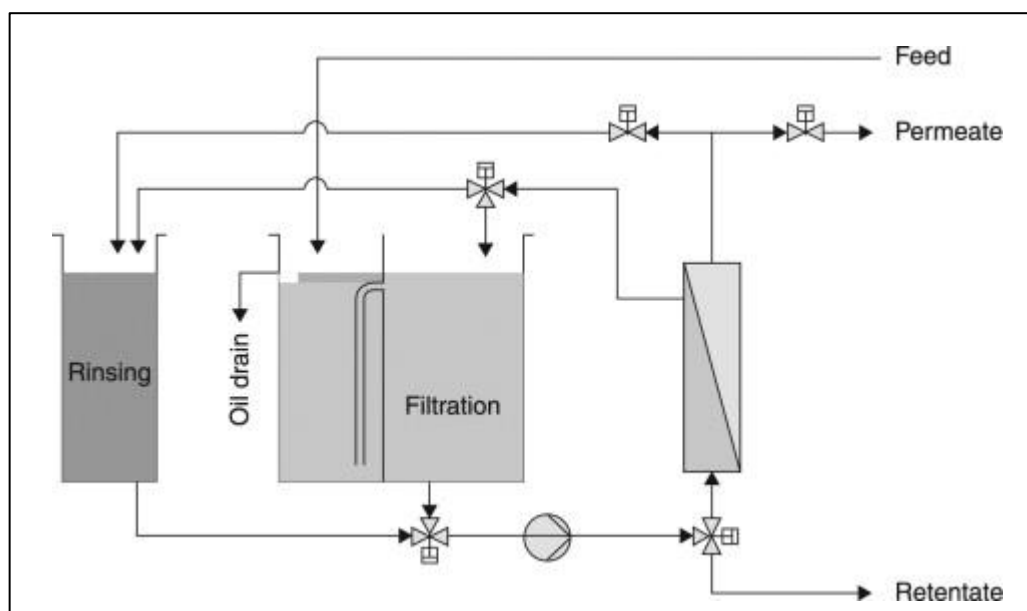
Figure 2.1: Scheme of Membrane Separation Process in Wastewater Treatment (Graff, 2012)

2.3.1.2   Disadvantages

The capital costs for membrane-based technology can be considered as exorbitant compared to the other conventional systems. Besides that, the current level of expertise of plant operators may not be up to par with the level required to handle this technology. Furthermore, the replacement costs of the fouled membrane are high and therefore require appropriate budgeting. Another underlying issue with membrane filtration is the disposal of the concentrate and waste streams (Mazille and Spuhler, 2019).

2.3.2 Chemical Precipitation

Another effective removal method of heavy metals from wastewater is by chemical precipitation. Many industries employ its use as it involves relatively low capital costs and is easy to operate (Yadav, Gupta and Sharma, 2019).

2.3.2.1 Process Description

Chemical precipitation process is commonly employed to eliminate undesirable heavy metals, hardness, and phosphorus from water. By adding a reagent through the mixing and dosing system as shown in Figure 2.2, the ionic equilibrium of the metallic ions and certain anions are altered to form precipitation that is insoluble in the water. These precipitates can then be easily removed by subsequent solids separation processes such as filtration, sedimentation, or coagulation. Preceding chemical precipitation, a chemical reduction process can be introduced to facilitate in changing the metal ions to a more easily precipitated form (Wang et al., 2005).
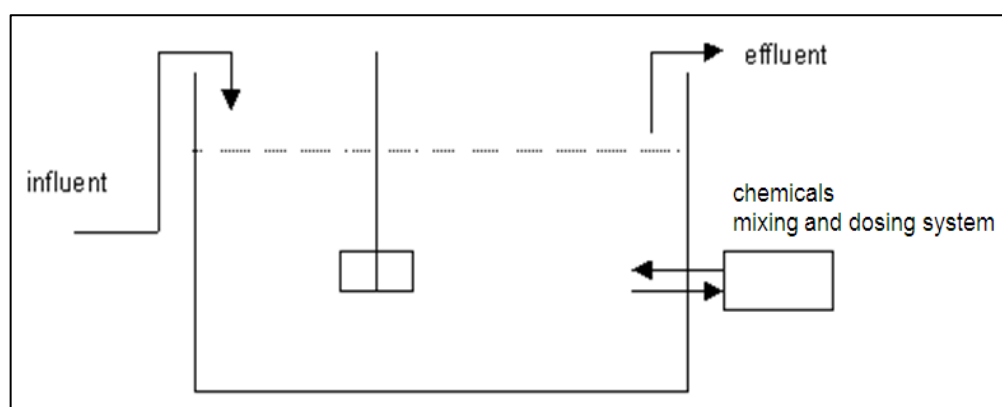
Figure 2.2: Method Diagram for Chemical Precipitation Process (EMIS, 2010a)

2.3.2.2 Disadvantages

A large quantity of reagent is usually needed due to the requirement of 1:1 cation to reagent ratio in the chemical precipitation process. This translates into additional costs for operation since reagents such as barium sulphate are quite expensive. Besides that, large amounts of sludge are produced through this process. For sludge that can be precipitated as a useful by-product, typical problems encountered include its high processing and treatment costs. This is because the sludge is regarded as a dangerous waste due to its high content of heavy metals (EMIS, 2010a).

2.3.3   Electrochemical Process

The major methods for electrochemical treatment of wastewater include the use of electrocoagulation, electroflotation, and electrooxidation.

2.3.3.1   Process Description

An electrochemical treatment unit comprises of cathodes and anodes installed parallel to each other. By switching on the electric power, the anode material is oxidized while the elemental metals of the cathode undergo reduction reactions. Based on the conditions imposed on the system, further reactions may occur and require the removal of the various contaminants in water through either electrocoagulation, electroflotation, and/or electrooxidation mechanisms (National Programme on Technology Enhanced Learning (NPTEL), 2019). A schematic diagram showing the use of an electrochemical process to treat the wastewater produced by the sugar industry is portrayed in Figure 2.3.
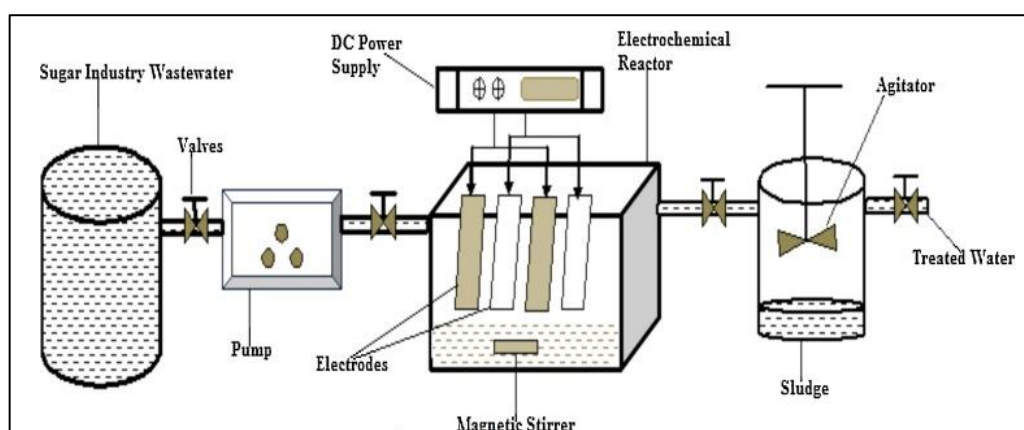
Figure 2.3: Diagram of the Electrochemical Process in the Treatment of Wastewater
from the Sugar Industry (Sahu et al., 2017)

2.3.3.2   Disadvantages

The regular replacement of the 'sacrificial electrodes' that are dissolved into the wastewater streams for the redox reaction process is a major limitation of this removal technique. Besides that, this method may not be economically viable in developing countries with limited access to electricity. There is also a loss of efficiency of the electrochemical unit due to the impermeable oxide film that forms on the cathode. Furthermore, the wastewater suspension must possess high conductivity for an effective separation to occur (Joseph, 2013).

2.3.4   Coagulation-Flocculation Process

Wastewater treatment is also extensively carried out by the process of coagulation which is immediately followed by flocculation.

2.3.4.1 Process Description

Coagulation involves adding a coagulant to the water to destabilize the colloids and suspensions through the neutralisation of charges. The destabilisation process will cause the polluting matter to bunch together. Subsequent to the coagulation process, flocculation takes place where it involves adding polymers to physically agglomerate the small and destabilized particles into larger sized clumps to ease the process of separating them from the water (Butani and Mane, 2017). The combined coagulation-flocculation process is depicted in Figure 2.4.
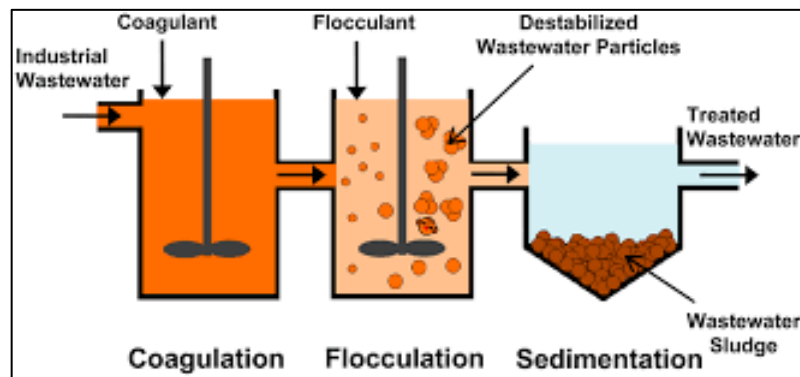
Figure 2.4: The Coagulation-Flocculation Processes for the Treatment of Industrial
Wastewater (Teh et al., 2016).

2.3.4.2 Disadvantages

The major drawback of this method is its high operating costs as there are instances where substantial amounts of coagulants and flocculants are required to meet the desired levels of separation. Another point of consideration is the escalating costs of the external processing of the physiochemical sludge formed, especially during the handling of wastewater of considerable volumes. Besides that, the selection of the dosage of chemicals for the process to function effectively is not that straightforward since wastewater has a composition that largely varies (EMIS, 2010b).

2.3.5 Ion Exchange

Besides being used in separation processes in areas such as food processing, medical research, chemical synthesis, agriculture, and mining, the ion exchange process is extensively used in water and wastewater treatment (Cobzaru and Inglezakis, 2015).

2.3.5.1 Process Description

A reversible chemical reaction takes place whereby the targeted ions contained in the wastewater solution is interchanged with an identically charged group of ionic species situated within the immobile acid or base exchange resins. Therefore, the contaminant ions will accumulate on the resin whereas the less harmful ions belonging to the resin are released to substitute the absence of the contaminants in the solution. A strong base or strong acid regenerant is used to discharge target ions to allow for the regeneration of the exchange capacity of the resin so that it may be reused on more of the original solution (Chen et al., 2006). The operating principles underlying the ion exchange mechanism is depicted in Figure 2.5.
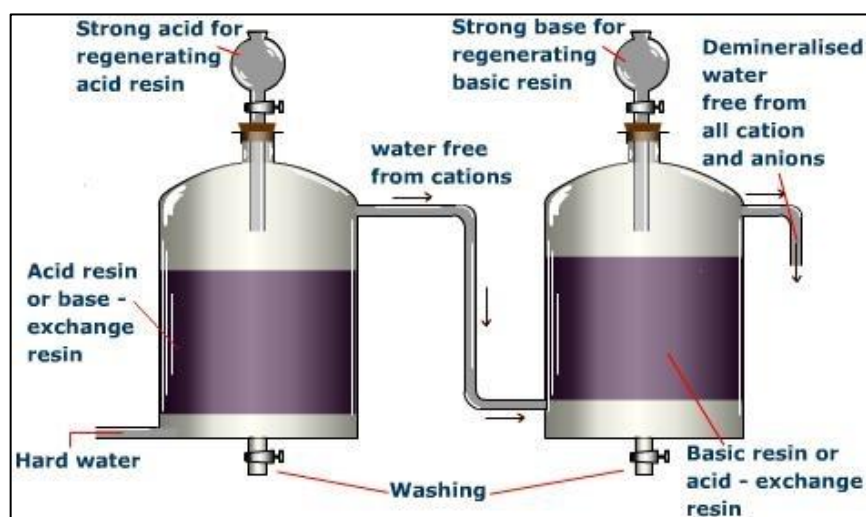
Figure 2.5: Operating Scheme of Ion Exchange Process (Home Water Purification Systems, 2019)

2.3.5.2 Disadvantages

There is a reduction in the exchange capacity of the resins due to the quick fouling or pollution by suspended material pollution and microbiology like bacteria that forms a layer of film on the resin. Furthermore, there are uneconomically high operating

costs involved in the disposal of the regeneration fluid after its use as it forms a major concentrate flow (EMIS, 2019).

2.3.6 Summary of Conventional Treatment Methods

The principal characteristics and disadvantages of each of the conventional treatment methods are tabulated in Table 2.4.

Table 2.4: Main Characteristics and Disadvantages of the Conventional Removal Methods of Heavy Metal from Wastewater

Treatment Method	Main Characteristics	Disadvantages
Chemical precipitation	Formation and separation of insoluble precipitation	• High volumes of sludge produced • High sludge treatment costs
Electrochemical process	Involves the use of electrolysis	• Involves constant replacement of the sacrificial anodes • Formation of impermeable oxide film on cathode hinders efficiency
Coagulation-flocculation process	Adding of coagulants to destabilise particles and flocculants to agglomerate the particles.	• High consumption of chemicals • Large volume of sludge generation
Ion Exchange	Involves an immobile acid or base exchange resins	• Rapid fouling of resin by organic matter • High disposal cost of regeneration fluid

2.4 Adsorption

Taking the disadvantages associated with each of the conventional methods discussed in Section 2.3 into consideration, the adsorption process has seen a rise in

popularity amongst researchers. This is because the process is easy and effective to set up whilst also involving the least amount of capital and operating costs particularly if regeneration of the adsorbent is performed in the system.

2.4.1   Process Description

Adsorption involves the transfer of particles (adsorbate) from a liquid or gas and the forming of a superficial monolayer of the particles onto the surface of an adsorbent (Crawford and Quinn, 2017). This adsorption process as shown in Figure 2.6 involves three main steps:

(i)   The first step is a process known as film diffusion. The target molecule traverses across the bulk fluid to the exterior of the adsorbent particle by first diffusing through the film of solvent surrounding the adsorbent.

(ii)   The next step is known as pore diffusion. The adsorbate molecule will move to an adsorption site located inside of the pore of the adsorbent.

(iii)   The final step is where the actual adsorption occurs. The adsorbate particles attach to the active sites of the adsorbent to form a single monolayer of the molecules.
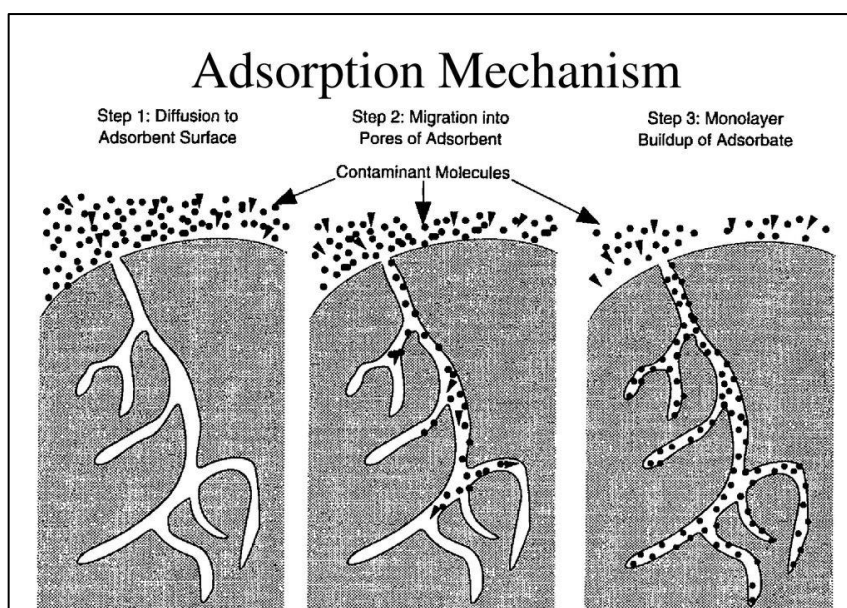
Figure 2.6: The Three Main Steps of the Adsorption Mechanism (Subbareddy, 2015)

Adsorption is categorised as either a chemical or physical process. The physical adsorption process is reversible and is mainly driven by van der Waals forces. It occurs primarily when the interparticle interaction forces between the adsorbent and solute are more significant than the forces that exist between the solvent and the solute. In contrast, chemical adsorption comprises of a chemical reaction taking place between the adsorbent particles and the adsorbate surface. Chemical adsorption is irreversible most of the times and is stronger than its physical counterpart (Hung et al., 2006).

2.4.2   Advantages

One of the plus points of the adsorption process is its flexible operation which will assist in the yield of high-quality treated effluents. Besides that, as mentioned in Section 2.4.1, the adsorption process is sometimes reversible which means that an appropriate desorption process can be incorporated into the process for the regeneration of the adsorbents (Fu and Wang, 2011). Furthermore, adsorption has advantages over the other water treatment methods which include a simpler design and lower investments involved with regards to the initial costs and size of land area required (Rashed, 2013).

2.5   The Use of Activated Carbon in Adsorption Process

Although there are numerous materials that can be employed in the process of adsorption, activated carbon in powdered and granular form are by far the most commonly utilised adsorbents in treating domestic and industrial wastewater. The wide applicability of activated carbon for treating wastewater is mainly due to its large microporous and mesoporous volumes that result in high surface areas, their non-polar character, and economic viability (Rashed, 2013).

Activated carbon adsorption takes place in conjunction with activated sludge treatment in an aeration tank. Activated carbon is dosed in the tank depending on the required amount needed to reduce the level of water pollution. The recycling of activated carbon takes place with the activated sludge but fresh activated carbon needs to be continuously added to the system. Figure 2.7 illustrates the schematic representation of the process of activated carbon treatment.
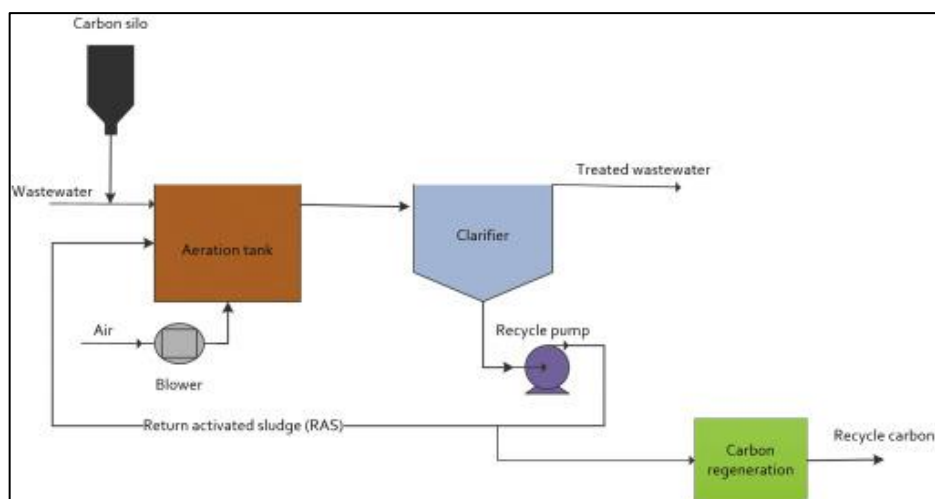
Figure 2.7: Schematic Representation of Activated Carbon Treatment (Jafarinejad, 2017)

2.5.1   Disadvantages of Activated Carbon

Activated carbon production is energy-intensive and commercially-expensive as it involves high temperatures during the pyrolysis and activation stages of the process (Ceyhan et al., 2013). Besides that, the continuously depleting source of coal-based activated carbon will also result in the rise of prices of this adsorbent (Fu and Wang, 2011).

Furthermore, in some adsorption systems, the adsorbent regeneration may not prove to be economically viable, so the activated carbon must be destroyed in an incinerator where its emissions to the atmosphere may pose environmental risks (EMIS, 2010a).

In addition, skilled labour is occasionally required during the monitoring of the removal performance over time of the activated carbon involved in the point-of-entry (POE) or point-of-use (POU) equipment units (Mazille and Spuhle, 2019).

2.6   Biosorption and its Mechanism

Based on the drawbacks of the general adsorption process, the need for a more economical, easily available, and environment-friendly adsorbent to sequester heavy metal ions from industry effluents has given rise to the field of biosorption.

Based predominantly on passive transport mechanisms, biosorption is a simple, physicochemical process. It involves the rapid and reversible process of binding the metallic ions (biosorbates) from the bulk fluid onto the functional groups

located on the cellular surface structure of an adsorbent of biological origin (biosorbent) (Özer, Özer and Ekiz, 2005).

The binding of these ions can occur through a single mechanism or by a sequence of several processes. The forces governing the adhesion of the ions can be physical by means of van der Waals forces or electrostatic interactions. Conversely, the nature of the forces can be chemical by means of the ionic exchange of protons or metal cations bounded to the surface. The other biosorption pathways include chelation, complexation, precipitation, and adsorption. To facilitate in the binding process, the biosorbents comprise of functional or chemical groups like phosphate, amino, carboxylate, hydroxyl, and sulphate which permit the attraction and sequestering of these metal ions (Crist et al., 1981).

As discussed in Section 2.4.1, a consensus by researchers is reached where three steps occurring consecutively describe the adsorption process most accurately (Al-Duri, 1996). These principles of adsorption can be adapted for the biosorption of metal ions by a biosorbent particle acting as an individual cell as illustrated in Figure 2.8 and they are described in the following primary steps (Abbas et al., 2014):

(i) External mass transfer of metallic ions from the bulk fluid to the liquid film surface of the biosorbent cell.

(ii) The ionic transport of the particles from the film of boundary liquid to the biosorbent cell surface.

(iii) The movement of the heavy metal from the surface of the cell to the binding active sites located within the cell through either physical adsorption, complexation, or surface precipitation.

(iv) The interactions that occur between the heavy metal particles and the active binding sites.
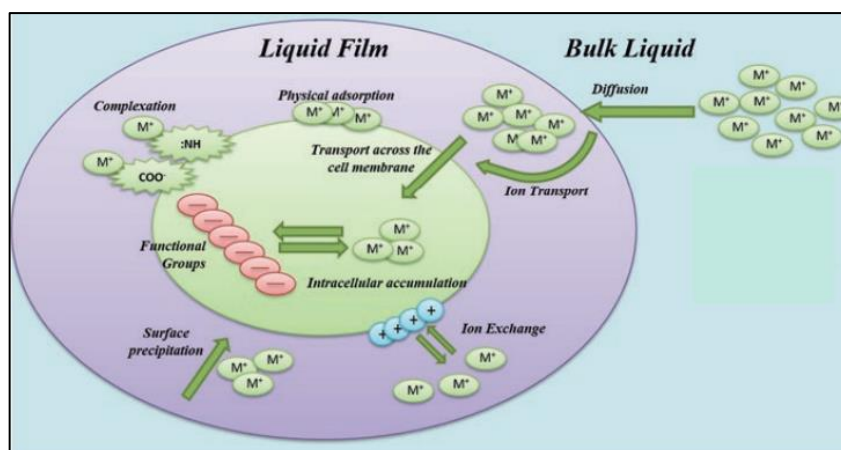
Figure 2.8: Schematic Diagram of the Biosorption Mechanism of Heavy Metals
(Abbas et al., 2014)

The external diffusion and adsorption processes occur rapidly and are, therefore, not the rate-limiting steps of biosorption. Alternatively, it is well established that the rate-limiting step is actually the intra-particular diffusion which can be modelled using the Weber and Moris equation (Papirio et al., 2017).

When the metallic ion concentration of the bulk fluid no longer varies with time, adsorption equilibrium is said to be achieved. The factors that will influence the time necessary to achieve adsorption equilibrium are the particle size and diffusivity coefficients of the metal ions (Padmavathy, 2008).

2.6.1   Advantages

The important advantage of utilising biosorption as a removal technique of heavy metals in wastewater is its cost-effectiveness as the adsorbent materials are being produced from naturally-accessible and renewable waste products (Foo et al., 2012). It also shows great potential to be commercialised as it involves low capital and operational costs. There is also a lack of need for additional nutrient supply and highly-priced reagents that contribute to space and disposal problems (Abbas et al., 2014).

Besides that, biosorption is a simple operation as it only involves a single-stage process. Furthermore, biosorption possesses high removal rates as it involves rapid kinetics and is extremely selective in removing the desired heavy metals. From an environmental standpoint, the biosorption process produces only small quantities of sludge and does not cause an increase in the chemical oxygen demand (COD) of

water. The biosorption process also has regeneration capabilities due to the reversibility of the process (Kanamarlapudi, Chintalpudi and Muddada, 2018). The lack of the aforementioned advantages is the huge limitation that hinders most of the conventional removal techniques mentioned in Section 2.3.

Other advantages such as it does not promote any undesired cellular growth, does not impose any toxic effects, and is not restricted by any metabolic pathways make it a very suitable candidate for wastewater treatment (Kanamarlapudi, Chintalpudi and Muddada, 2018).

2.6.2 Factors Affecting Biosorption Mechanism

There are many factors that play a role in the rate of metallic uptake onto the biomass surface which will ultimately determine the overall biosorption efficiency. The mechanisms of biosorption of metals are controlled and characterized by the following key factors:

(i) The chemical properties, stereochemistry characteristics, and coordination behaviour of the metal ions such as their molecular weights, oxidation numbers, and ionic radii of the targeted metal species (Kanamarlapudi, Chintalpudi and Muddada, 2018).

(ii) The structure or nature of the biomass (Abbas et al., 2014).

(iii) Functional groups present on the binding site.

(iv) The parameters like the initial pH of the solution, the operating temperature, initial concentration of the metallic ions, the dosage and size of the biomass, as well as the presence of other coexisting metallic ions (Papirio et al., 2017).

(v) The number of binding sites available on the biosorbent.

For the scope of the current study, more emphasis will be placed on the effect that parameters have on the metallic uptake of the biosorbent.

2.6.3 Limitations of Biosorption

Although biosorbents have the advantages of being widely soured and low cost as well as offering rapid adsorption, they are limited to small-scale applications as the research on the subject is still in the theoretical and experimental stages. There are also challenges associated with separating the biosorbents from the solution after

adsorption (Fu and Wang, 2011). Despite the existence of commercialised biosorbents to sequester metallic ions from aqueous solutions, none of them have been applied in any industrial facility to date (Park, Yun and Park, 2010).

2.6.4 Biosorbents used in Nickel Removal

Biosorbents are typically sourced from either living or dead biomass. Biosorbents that are typically used include plant-based materials, microorganisms, wastes generated by agriculture or industrial processes, biopolymers, and many more (Kanamarlapudi, Chintalpudi and Muddada, 2018).

There is a large collection of research studies that have either been reported or are currently being conducted on the biosorption of nickel. Biomasses of various types have displayed good results for the removal of nickel which means the process of biosorption has a high potential of being applied in large-scale wastewater treatment. Sorted according to categories, the nickel uptake capacities (q) of some of the biosorbents studied in previous research along with their respective operating pH, temperature (T), initial nickel concentration (C_o), biosorbent dosage (m), and contact time are outlined in Table 2.5.

Table 2.5: Nickel Uptake Capacities of Biosorbents at their Respective Experimental Operating Conditions

Category	Biosorbent	pH	T (°C)	C_o (mg/L)	m (g/L)	Time (min)	q (mg/g)	Reference
Bacteria	*Streptomyces coelicolor*	8.00	25.00	150.0	1.000	5.00	11.1	(Öztürk, Artan and Ayar, 2004)
	Streptomyces rimosus	5.00	25.00	500.0	3.000	120.0	32.60	(Selatnia et al., 2004)
	Bacillus laterosporus	5.00	25.00	50.00	4.000	120.0	44.44	(Kulkarni, Shetty and Srinikethan, 2014)
Fungi	*Aspergillus niger*	6.25	25.00	30.00	2.980	240.0	4.820	(Amini, Younesi and Bahramifar, 2009)
	Dried R. oligosporus	5.00	30.00	100.0	1.000	360.0	116.0	(Ozsoy and van Leeuwen, 2012)
	Polyporous versicolor	5.00	35.00	400.0	0.600	120.0	57.00	(Dilek, Erbay and Yetis, 2002)
Algae	Mixture of three algae	7.00	25.00	35.00	5.000	120.00	9.848	(Mohammed et al., 2019)
	Enteromorpha sp.	4.79	25.00	100.0	1.000	70.00	250.0	(Tolian, Jafari and Zarei, 2015)
	Marine macroalgae	5.00	30.00	500.0	5.000	120	181.2	(Kalyani, Srinivasa Rao and Krishnaiah, 2004)
Agricultural	Modified plantain peel	4.36	25.00	120.0	8.200	-	77.52	(Garba, Ugbaga and Abdullahi, 2016)
Waste	Lychee seeds	7.50	25.00	750.00	1.000	7200	66.62	(Flores-Garnica et al., 2013)

2.6.5   Factors Affecting Biosorption

As Table 2.5 has shown, the influence that certain factors have on the performance of a biosorbent in the removal of cationic contaminants from water should be taken into consideration. Past studies have shown that the temperature and the pH of the aqueous media directly affect the biosorption process. Additionally, the effectiveness of a biosorbent is heavily influenced by biosorbent dosage and initial concentration of the heavy metal. The current study will emphasise on the effects that initial nickel concentration, pH, and biosorbent dosage have on the results obtained from the biosorption studies.

2.6.5.1   Effect of Initial Nickel Concentration

The mass transfer resistance between the liquid film surface of the biosorbent cell and the bulk fluid is overcome by the driving force provided by the initial nickel ion concentration. Furthermore, there are more nickel ions available for biosorption at higher concentrations (Flores-Garnica et al., 2013).

Using *Phaseolus vulgarism* L. immobilized on silica gel, Akar et al. (2009) found that with increasing concentrations from 75 to 300 mg/L, the nickel uptake also rises as a result of a growing driving force. The surface of the biosorbent had active sites that interacted with the nickel ions present in the aqueous media which improved the capacity for biosorption. Beyond 300 mg/L, the nickel uptake was found to be relatively constant at 90.44 mg/g (Akar et al., 2009).

2.6.5.2   Effect of Biosorbent Dosage

Biosorbent dosage quantifies the number of binding sites available to bind with metal ions (Montazer-Rahmati et al., 2011). This parameter also gives an estimation of the cost of adsorbent per unit volume of the aqueous solution.

In a study of biosorption using protonated rice bran by Zafar, Nadeem and Hanif (2007), nickel uptake was 106.8 mg/g with a low dosage of 0.05 g but only an adsorption of 26.1 mg/g was achieved with a higher dosage of 0.25 g. The reduction in nickel uptake at high dosage is due to the decrease in nickel quantities adsorbed onto the unit mass of an adsorbent (Montazer-Rahmati et al., 2011). On the contrary, increasing the dosage of the biosorbent results in an increase in its removal efficiency as there are more adsorption sites present for adsorption.

2.6.5.3 Effect of pH

The pH of a solution determines the speciation of the metal ions that are present in the aqueous phase as well as the dissociation of functional sites that are active on the biosorbent surface (Srivastava, Agrawal and Mondal, 2015). As ion exchange between nickel ions and counter-ions on negatively-charged ionic groups is the dominant removal mechanism, the increase in competition between the protons and metal ions for binding sites will occur at low pH values. Conversely, the surface becomes negatively charged as well as the freeing up of functional active sites such as hydroxyl, carboxyl, and amino groups occurs when the pH of the aqueous environment is higher than the isoelectric point. This will enable the electrostatic attraction between the nickel ions and binding sites (Popuri et al., 2009). However, nickel ions can precipitate as hydroxides at higher pH values which will also hinder the biosorption process (Christoforidis et al., 2015).

Based on biosorption studies carried out on raw and pre-treated *Oedogonium hatei* in the pH range of 2.2 to 7.0, the nickel uptakes of both biosorbents were negligible between the pH of 2.0 to 4.0 whereas it increased in the range between 4.0 to 5.0. However, the uptake decreased beyond a pH of 5.0 (Gupta, Rastogi and Nayak, 2010).

Referring to the compilation of literature data shown in Table 2.5, it was concluded that the optimum pH range that facilitates in removing nickel is from 4.36 to 8.00 depending on the type of biosorbent (Gürel, 2017),

2.6.6 Fruit Peel Waste as a Biosorbent

The tropical climate of Malaysia promotes the diversity of the agro-industry through the cultivation of a wide range of crops. The growth of the industry has led to the increased levels of harvesting, handling, consumption, and the inevitable biomass generation of the products of agriculture (Pathak, Mandavgane and Kulkarni, 2017). In the present day, fruit peel waste is gaining in popularity in its use as a biosorbent because of its easier accessibility compared to other sources of biomass (Duru and Duru, 2017). Furthermore, it exhibits high potential as a biosorbent due to the presence of large porous structure and high fixed carbon content (Bhatnagar and Minocha, 2010).

2.6.6.1 Background of Longan Fruit and its Potential as a Biosorbent

Dimocarpus longan commonly referred to as longan, is part of the *Sapindaceae* family of flowering plants. Longan which is an economically important subtropical and tropical plant is widely grown in regions such as Taiwan, China, and Southeast Asian countries like Malaysia, Thailand, Vietnam, and the Philippines (Tseng et al., 2013). Besides that, the longan crops are also grown in other areas like Queensland and New South Wales in Australia as well as California and Florida in the United States (Rangkadilok et al., 2007).

These sweet and juicy fruits are popular among people from all over the world, leading to its high growth in market demand (Tang et al., 2019). Longans are mostly consumed as fresh fruits where their pulp is the only edible part. The fruit peel and seed of the longan fruit are typically discarded as agricultural and domestic waste which contributes in the long run towards the concerning solid waste disposal problem at a larger scale. This is because these fruit peels and seeds are disposed without any plan of practical reuse annually (Li and Tao, 2016).

Owing to its extensive availability and environmental benignity, the longan fruit peel has the prospects to be a reliable biosorbent in the removal of contaminants in wastewater (Wang et al., 2016).

Furthermore, the peel of this fruit is known to be composed of high contents of lignin, hemicellulose, and cellulose. Cellulose is a type of polysaccharide that can contain hundreds to several thousands of *D*-glucose units that are *β*-linked to each other to form linear chains, which contribute towards its sorption properties. Its surface structure also contains functional groups such as phenolic, methoxyl, carbonyl, and carboxyl that will enhance its intrinsic affinity towards heavy metals ions contained within aqueous solutions (Huang, Li and Li, 2010).

2.6.6.2 Longan Biosorbent in Past Research

To the author's knowledge, only a handful of work has been dedicated to investigating the potential of longan as a biosorbent in wastewater treatment. Previous studies include the work of Wang et al. (2016) that reported 141.04 mg/g as the maximum adsorption capacity of longan peel in the treatment of aqueous solutions contaminated by methylene blue.

Another study using longan peel as a biosorbent to remove lead and mercury ions had shown impressive removal efficiencies of 92.1 and 99.1 % respectively. The

batch adsorption tests were conducted with a dosage of 300 mg of longan peel in 25 ml of 20 mg/L initial ion concentration for two hours at 20 $^{\circ}$C (Huang, Li and Li, 2010).

Research has also been done using the column method where the performance of longan peels and seeds in removing copper (II) ions contained within aqueous solutions were evaluated. The biosorption capacities for peel and seed were 7.513 mg/g and 3.734 mg/g respectively for optimised conditions of pH 3, biosorbent dosage of 0.5 g, and particle size of 250 μm (Kurniawati et al., 2016).

The use of longan peels in removing methylene blue and basic magenta dyes from synthetic solutions was also the subject of past research. Increasing trends of adsorption capacity were observed with an increase of initial pH from 2.2 to 5.5, a decrease of biosorbent dosage, and a decrease in particle size (Li and Tao, 2016).

None of the reviewed articles involved the use of longan peels as a biosorbent to remove nickel ions present in aqueous solutions. Furthermore, response surface methodology was not a tool employed in the analysis of experimental data by any of the past studies. To fill this research gap, the present study investigated the performance of longan peels in its natural form with regards to its efficiency in removing nickel ion contaminants from aqueous solutions. The adsorption performance of activated carbon was evaluated simultaneously to determine the applicability of substituting activated carbon with longan peels in an actual wastewater treatment plant. In addition, optimisation of the initial nickel concentration, biosorbent dosage, and pH to yield the maximum removal efficiency of longan peels was determined by use of response surface methodology.

2.7   Modelling of Adsorption Isotherms

The quantitative knowledge of the interaction between the adsorbent and the adsorbate, the affinity of the adsorbents at the equilibrium stage, the properties of the surface, as well as the mechanism of the process can be deduced from the physical, chemical, and mathematical considerations of the adsorption isotherm (Sohbatzadeh et al., 2016). The strategies involved in implementing an adsorption system into an actual wastewater treatment plant can be based on the evaluations of the equilibrium data. Two of the most widely-used adsorption isotherms, namely the Langmuir and Freundlich equations were applied in the modelling of the adsorption equilibrium.

2.7.1 Langmuir Isotherm

Proposed in 1932 by Irving Langmuir, the Langmuir adsorption model is based on the following assumptions (Bushra, Ahmed and Shahadat, 2017):

(i) The adsorbent surface has active sites that are all identical to each other.

(ii) The adsorption process will only take place on the specific and finite number of active sites that are confined to the adsorbent surface.

(iii) There are no lateral interactive effects that occur among the adjacent adsorbed molecules.

(iv) A single layer of adsorbed molecules is formed on the adsorbent surface.

Based on the aforementioned assumptions, Langmuir adsorption model in its non-linear form is shown to be as Equation 2.1 (Liu et al., 2019):

$$q_e = \frac{q_m K_L C_e}{1 + K_L C_e} \tag{2.1}$$

where

q_e is the adsorption capacity of the adsorbent at equilibrium conditions, mg/g,

q_m is the adsorption capacity required to form a monolayer, mg/g,

K_L is the free energy of adsorption constant,

C_e is the concentration of the adsorbate in the fluid achieved at equilibrium, mg/L.

Furthermore, the dimensionless constant associated with the Langmuir isotherm known as the separation factor, R_L is essential to provide a better description of the favourability of adsorption. It can be evaluated by using Equation 2.2.

$$R_L = \frac{1}{1 + K_L C_o} \tag{2.2}$$

where

C_o is the concentration of the adsorbate particles present in the bulk fluid before adsorption, mg/L.

2.7.2   Freundlich Isotherm

The first-ever isotherm to represent the adsorption process of a solute from a solution to a surface of a solid was proposed by Freundlich in 1906 and was presented as an empirical equation. The applicability of the model extends towards multilayer, non-ideal adsorption on heterogeneous surfaces of adsorbents (Liu et al., 2019).

In terms of adsorbate concentration, the linearised Freundlich model can be described using Equation 2.3 (Sahu and Singh, 2019).

$$q_e = K_F C_e{}^{1/n}$$ (2.3)

where

K_F is the constant that correlates to the relative adsorbent adsorption capacity, mg/g,

$1/n$ is the measure of the adsorption intensity of the adsorbate.

The n value serves as an indicator of the degree of surface heterogeneity and the distribution of the adsorbed particles on the adsorbent surface (Keçili and Hussain, 2018). Favourable adsorption of the adsorbate on the adsorbent surface is related to n values ranging from 1 to 10. Strong forces of adsorption within a system are indicated by high fractional values of $1/n$. The magnitude of this fraction also suggests the capacity of the adsorbent-adsorbate system (Liu et al., 2019).

2.8   Response Surface Methodology (RSM)

Established by Box and Wilson in the early 1950s, response surface methodology (RSM) is a common tool used in ascertaining the optimal conditions of a process through the design of experiments. The input variables which can be controlled are the independent factors whereas the resulting outputs are the response variables.

2.8.1   Regression Analysis

In order to approximate stochastic models, RSM features a compilation of statistical and mathematical techniques that make use of regression analysis based on low-degree polynomials as shown in Equation 2.4.

$$Y = f(X_1, X_2, X_3, \ldots, X_k) + e \qquad (2.4)$$

where

Y is the experimental response value,

f is the function of cross-product of the polynomial terms,

$X_1, X_2, X_3, \ldots, X_k$ are the input variable values,

e is the error term.

The second-order quadratic model as shown in Equation 2.5 is the more commonly used form of the polynomial function. The first summation in the equation is the linear part, the second summation is the quadratic part, and the third summation is the product of the variables in pairs. Regression analysis is utilised to compute the coefficient of the offset term (b_0), linear terms (b_i), and interaction effects (b_{ii} and b_{ij}) (Lorza et al., 2018).

$$Y = b_0 + \sum_{i=1}^{n} b_i \cdot X_i + \sum_{i=1}^{n} b_{ii} \cdot X_i^2 \sum_{i=1}^{n-1} \sum_{j=i+1}^{n} b_{ij} \cdot X_i \cdot X_j + e \qquad (2.5)$$

2.8.2 Optimisation Based on Desirability Function

The numerical optimisation approach involves determining one point or more that achieves the objective of the function (Lin et al., 2018). The goals set for each of the factors and the response can be either to maximise, minimise, target, or set the value to be within a certain range. Furthermore, the response can be set as none while the factor can be set to be a specific value. Each of the factors and response must have a minimum and maximum level specified for them.

The shape of the desirability function is adjusted based on the weight that is allocated to each goal. The overall desirability function is a combination of all the goals. Desirability is described as an objective function that can hold values ranging from zero when the parameters are outside of the limits to one when the parameters achieve the goal. For the current study, the aim of optimisation is to maximise the removal performance of the adsorbent. The goal seeking function of the program starts at a random starting point and then moves up the steepest slope to a maximum value. Due to the various combination of goals in the overall desirability function

and the response surfaces curvature, two or more maximum points can be determined (Sadhukhan, Mondal and Chattoraj, 2016).

2.8.3   Response Surface

The response surface (RS) represents the graphical illustration of the response of the independent factors. These graphs ease in the visualisation of the response behaviours with every factor level and with a combination of the factors (Pelegri and Tekkam, 2003). It is useful in ascertaining the influence that the various factors have on the system and the interaction effects that occur between them through the analysis of the response values in the experimental design (Liu et al., 2016).

2.8.4   Analysis of Variance (ANOVA)

Assuming that the precision of the model is high, the Prob. $> F$ or p-value which is the probability of obtaining a result that equals or exceeds the observed values can be calculated by analysis of variance (ANOVA). When there are no terms in the model that exceeds the level of significance of $\propto = 0.05$ and the Prob. value is bigger than the F-value, the model is deemed to be acceptable at a confidence interval of (1-$\propto$).

2.8.5   Advantages of RSM

One of the major merits of using RSM is the fewer number of experiments that are required to interpret the factors. Whenever laboratory studies are upscaled to fit into an industrial system, the costs for the chemical materials, time, energy, and labour are expected to be lessened through the use of RSM. Furthermore, the RSM approach allows for a more comprehensive study of subjects that are insufficiently-researched and have a lack of data (Ozturk et al., 2017). RSM also finds usefulness in identifying and evaluating the interactive effects between all the variables responsible for adsorption to augment the adsorption isotherms studies (Oghenejoboh, 2018).

CHAPTER 3

METHODOLOGY AND WORK PLAN

3.1 Chemical Reagents and Materials

The chemical reagents and materials utilised throughout the duration of carrying out the experiments along with their respective purposes are listed in Table 3.1.

Table 3.1: Chemical Reagents and Materials Utilised

Chemical Reagents /Materials	Purpose
Waste peels of longan	Biosorbent
Commercial activated carbon	Adsorbent
Nickel nitrate, Ni $(NO_3)_2$ crystals	Preparation of nickel stock solution
Filter paper	Filtration of the samples after the batch adsorption test
Hydrochloric acid, HCl fuming 37 % solution	Diluted in water for acidic pH adjustment
Sodium hydroxide, NaOH pellets	Dissolved and diluted in water for alkaline pH adjustment
65 % nitric acid solution	Diluted for preparation of calibration standards and samples for ICP-OES analysis

3.2 Equipment Involved

The instruments involved along with their respective functions have been summarised in Table 3.2.

Table 3.2: Equipment Involved and their Purpose in the Study

Equipment	Purpose
Oven	Drying of the waste peels
Food processor	Grinding the waste peels to smaller pieces
Mechanical grinder	Pulverising the waste peels after drying
300-micron mesh	Sieve the grounded waste peels to finer particle sizes
Inductively coupled plasma optical emission spectrophotometer (ICP-OES)	Determining the concentration of nickel in the aqueous solutions after the batch adsorption tests
Shaking incubator	To provide the desired temperature and agitation speed required for the batch test
Fourier Transform Infrared (FTIR) Spectrometer	Analysing the functional groups present on the biosorbent and activated carbon surface
Analytical balance	To measure the desired biosorbent and activated carbon dosages
pH meter	Measurement of the pH during pH adjustment

3.3 Flowchart of Work Plan

The flowchart for the work plan is shown in Figure 3.1. The first steps include the preparation of the longan peel biosorbent, the activated carbon, and the nickel stock solution. The surface of the biosorbent and activated carbon were characterised using FTIR. Both the biosorbent and the activated carbon were subjected to batch adsorption studies in which the parameters namely, initial nickel concentrations, dosage, and pH were manipulated based on the design matrix. The most suitable adsorption isotherm for both longan peel and activated carbon were carried out based on the optimised initial nickel concentration, pH and adsorbent dosage.
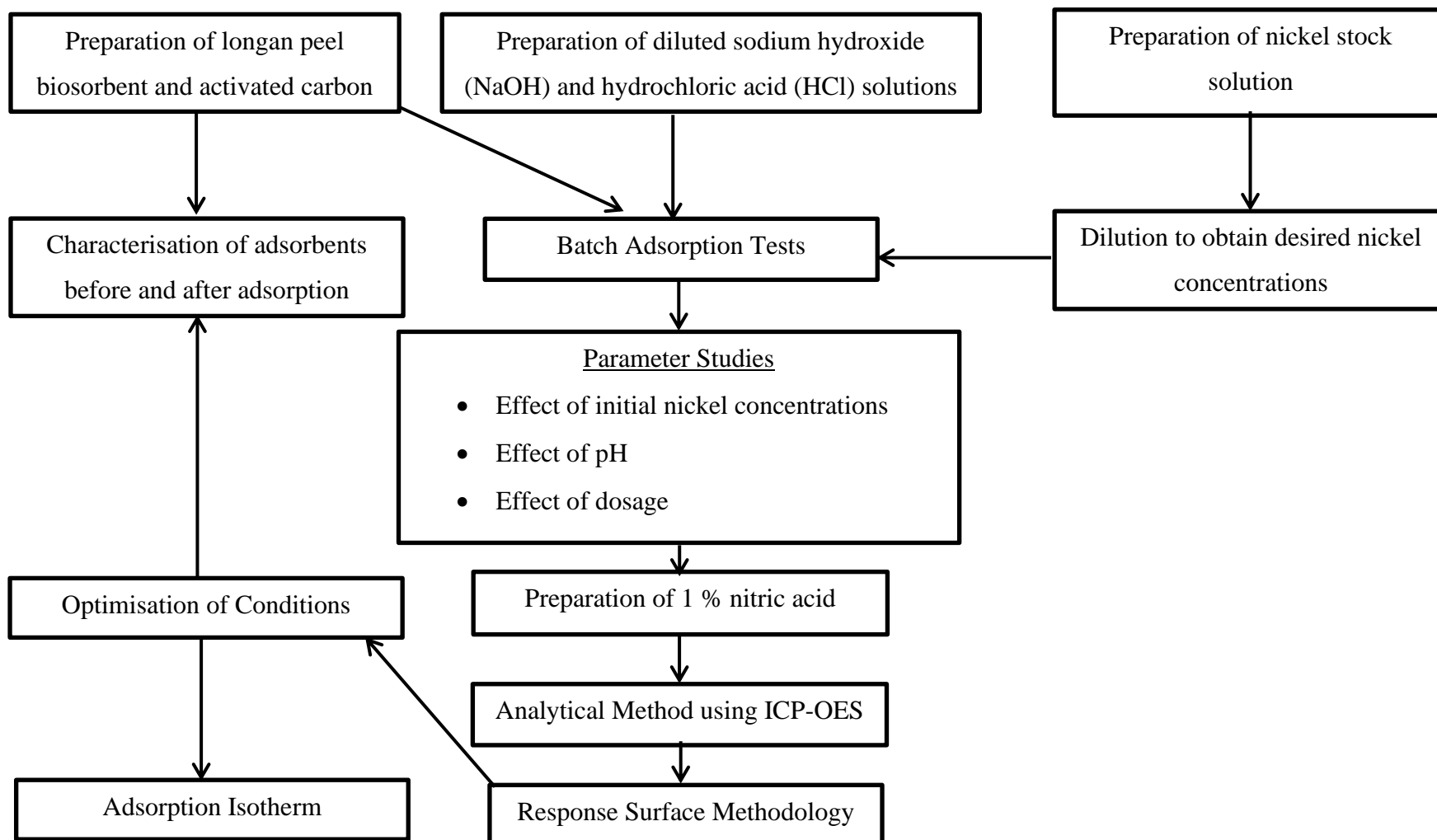
Figure 3.1: Overall Experiment Flowchart

3.4 Preparation of Longan Peel

The longan fruits were purchased from a nearby market. The waste peels of the longan fruits were collected and ground into smaller pieces using a food processor. The peels as shown in Figure 3.2 were then washed repeatedly using water to remove any traces of dirt and residues while the excess water was drained away. After that, the peels then underwent a drying process overnight in a convection oven at about 80 °C as illustrated in Figure 3.3 to reduce their moisture content and achieve a constant weight. Next, the dried fruit peels were pulverized using a mechanical grinder shown in Figure 3.4 and then passed through a 300-micron mesh as depicted in Figure 3.5 to create the final applicable biosorbent.

Figure 3.2: Ground and Washed Longan Waste Peels

Figure 3.3: Longan Peels Dried Overnight at 80 °C

Figure 3.4: Grinder to Pulverise the Longan Peels into Finer Particle Sizes

Figure 3.5: Use of a 300-micron Mesh to Sieve the Longan Peels

3.5　　　Preparation of Activated Carbon

Activated charcoal powder of ~100 particle size intended for use in research and development (R&D) was supplied by Sigma Aldrich. The powder has a relative density of 1.8-2.1 g/cm^3 and is insoluble in water to permit the adsorption of water-soluble adsorbates onto its surface.

3.6 Preparation of Nickel Stock Solution

The synthetic nickel (II) solution was prepared by dissolving 3.113 g of nickel nitrate crystals in distilled water to produce a 1000 mg/L nickel stock solution.

3.7 Characterisation using Fourier Transform Infrared (FTIR) Spectroscopy

The FTIR analyses were conducted on the adsorbents as shown in Figure 3.6 before and after the batch adsorption tests to determine which functional groups are present on the surfaces of the longan peel biosorbent and the commercial activated carbon.

Figure 3.6: FTIR Analysis of Adsorbent

3.8 Response Surface Methodology (RSM) Modelling

The combined effect of the three design variables, namely initial nickel concentration (A), adsorbent dosage (B), and pH (C) on the percentage nickel removal was modelled by applying RSM, using Box-Behnken design (BBD) as a basis.

The BBD-proposed matrix for the experimental design as tabulated in Table 3.3 was generated by Design Expert 11.0 after the range of each independent variable was inputted into the software. The chosen range for the initial nickel concentration (10 mg/L to 300 mg/L) is based on the nickel concentrations in industrial effluents from Table 2.2 whereas the pH range of 2 to 8 was selected to understand the effects that acid and basic conditions have on adsorption performance. On the other hand,

the range of adsorbent dosage which is between 1 g to 10 g is slightly larger than the values reported in past literature to ensure that equilibrium conditions were achieved within the contact time of three hours. The design matrix in Table 3.3 was generated and the experimental runs were randomly performed to ensure that the effect of unexplained variability were minimized. The design matrix consists of 17 experimental runs with the inclusion of five replications of the central points.

Table 3.3: Box-Behnken Design Matrix of Independent Variables

Run Order	Factors		
	A: Initial Nickel Concentration (mg/L)	B: Adsorbent Dosage (g)	C: pH
1	10.00	10.00	5.000
2	155.0	5.500	5.000
3	155.0	5.500	5.000
4	300.0	5.500	2.000
5	155.0	1.000	8.000
6	155.0	10.00	2.000
7	155.0	1.000	2.000
8	300.0	1.000	5.000
9	155.0	5.500	5.000
10	300.0	5.500	8.000
11	155.0	5.500	5.000
12	10.00	1.000	5.000
13	300.0	10.00	5.000
14	10.00	5.500	8.000
15	155.0	5.500	5.000
16	155.0	10.00	8.000
17	10.00	5.500	2.000

3.9 Batch Adsorption Studies

The adsorption of nickel by the longan fruit peel and activated carbon were studied by batch method at a fixed temperature of 25 °C. 250 mL conical flasks were used to contain 100 ml of Ni (II) solutions with concentrations of either 10, 155, or 300 mg/L. Using the nickel stock solution, simple dilution was conducted to prepare the desired

concentrations of the nickel solution. These solutions were dosed with adsorbents of either 1.0, 5.5, or 10.0 g which were measured using an analytical balance. The adsorption was conducted for three hours in a shaking incubator at a constant speed of agitation of 180 rpm.

The adjustments for the initial pH values of either pH 2, 5, or 8 were done by using sodium hydroxide or hydrochloric acid solutions wherever necessary. 500 ml of diluted HCl solution was prepared by diluting about 4 ml of HCl fuming 37 % in distilled water. On the other hand, 500 ml of dilute NaOH solution was made by dissolving about 2 g of NaOH pellets in distilled water. Using a glass dropper, appropriate additions of NaOH and HCl solutions to the nickel solution were done to obtain the desired initial pH as measured by a pH meter.

3.10   Analytical Method

50 mL solutions of a blank and five calibration standards with nickel concentrations of 5 to 30 mg/L were prepared to plot the calibration curve for ICP-OES analysis. Furthermore, quality control tests were also performed on a blank and a 25 mg/L sample to ensure that the calibration standards and instrument performance were at acceptable levels. Based on the calibration curve illustrated in Figure 3.7, the coefficient of determination or R^2 value is 0.999944 which signifies that the curve fits the calibration points well and can, therefore, be utilised to evaluate the unknown concentrations of the nickel ions in the filtered samples obtained from batch adsorption tests.
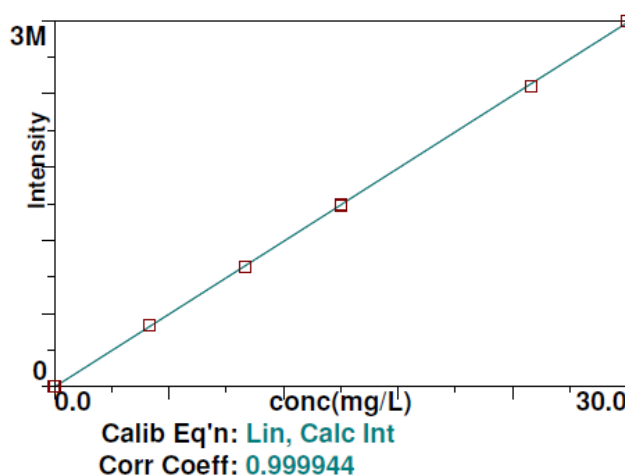
Figure 3.7: Calibration Curve for ICP-OES Analysis of Nickel (II) Ions

At the conclusion of every run of the batch tests, the samples were first filtered using filter papers and then with syringe filters to ensure that the filtrates were completely free from any adsorbent residue. They were then stored in centrifuge tubes and then diluted 1:10 in 1 % nitric acid solution to ensure that the calibration standards and samples have a matching matrix. The analysis was performed using the emission line of 231.604 nm.

Using the results obtained from ICP-OES analysis, the nickel uptake by the longan peel biosorbent and the commercial activated carbon (q_t in mg/g) were computed using Equation 3.1.

$$q_t = \frac{(C_o - C_f)V}{m}$$
(3.1)

where

C_o is the nickel ions concentration in the solution at the beginning of the batch adsorption test, mg/L,

C_f is the nickel ions concentration in the solution at the end of the batch adsorption test, mg/L,

V is the total volume of the aqueous solution in the conical flask, L,

m is the dosage of the biosorbent or activated carbon, g.

Besides, the removal efficiencies of nickel ions by the longan peel biosorbent and the activated carbon were also calculated using Equation 3.2:

$$Removal\ efficiency\ (\%) = \frac{(C_o - C_f)}{C_o} \times 100\ \%$$
(3.2)

3.11   Adsorption Isotherm

Preparation of a series of 100 ml volume of solutions containing nickel ion concentrations that range from 10 to 300 mg/L was carried out. Using these solutions, the batch adsorption tests will be conducted at the optimised pH and adsorbent dosage as determined by RSM to verify the validity of the Freundlich and Langmuir isotherms. After the elapsed time, the nickel ion content of the solutions was

measured using ICP-OES and the uptake of nickel ions at equilibrium, q_e was calculated based on Equation 3.3 which is a slight modification of Equation 3.1.

$$q_e = \frac{(C_o - C_e)V}{m}$$ (3.3)

where

C_e is the nickel ions concentration in the solution at equilibrium state, mg/L.

CHAPTER 4

RESULTS AND DISCUSSION

4.1   Characterisation Studies

The Fourier-transform infrared spectroscopy (FTIR) spectra of the longan peel biosorbent and activated carbon were analysed to establish which functional groups were associated with the adsorption process. The peaks in the longan peel biosorbent spectra were compared with the FTIR absorbance bands of spectra obtained from various biomass study. For the case of activated carbon, the peaks were compared with the "IR Spectrum Table and Chart" provided by Sigma-Aldrich (2020).

4.1.1   FTIR Spectra of Longan Peel

Figure 4.1 shows the stacked FTIR spectra of longan peel before and after the biosorption process. Before biosorption, it was observed that there is a significant and broad peak at 3290 cm^{-1} which matches with stretching vibrations of –OH. The adsorption peak at 2918 cm^{-1} may be correlated with a series of C–H vibrations in either the functional groups of –CH_2– or –CH_3 (Wang et al., 2016). Furthermore, the characteristic peak that was observed at 1609 cm^{-1} may be assigned to vibrations from an aromatic ring with stretching from a C=O group. Additionally, the wavenumber 1316 cm^{-1} has a peak that might correspond to –CH_2– wagging. Besides, the peaks at 1230 cm^{-1} can be associated with C–C with C–O stretching whereas the peak at 1019 cm^{-1} most likely corresponds to C=C, C–C–O, and C–O stretching.

The spectrum after biosorption has similar peaks to the ones observed before biosorption. After biosorption, the further broadening of the peak associated with the stretching vibrations of –OH at 3323 cm^{-1} may be due to the water molecules being adsorbed onto the surface of the longan peel. The other aforementioned peaks have slightly lower transmittance, indicating that the nickel ions may have form bonds with the functional groups and cause changes in the intensity of those peaks.

Based on Table 4.1, it is observed that a significant portion of the functional groups observed in the spectra involve the oxygen atom. According to Huang, Li and Li (2010), these groups are the sites where adsorption of heavy metal ions mainly occurs as they own lone pairs of electrons that can effectively interact with metal ions for metal-complex formation. All the functional groups in Table 4.1 belong to

the polymer groups of cellulose, hemicellulose, and lignin. These polymers are known to enhance the ability of a structure to extract ions of heavy metals from aqueous solutions (Huang, Li and Li, 2010).

Table 4.1: Polymer Groups Associated with FTIR Absorbance Bands (Xu et al., 2013)

Wavelength/ cm^{-1}	Functional group	Chemical Structure
3290	–OH stretching	Lignin
2918	C–H stretching	Lignin
1609	C–C vibrations in aromatic ring and C=O stretching	Lignin
1316	–CH$_2$– wagging	Hemicellulose, cellulose
1230	C–O with C–C stretching	Lignin
1019	C=C, C–C–O, and C–O stretching	Cellulose, hemicellulose, lignin
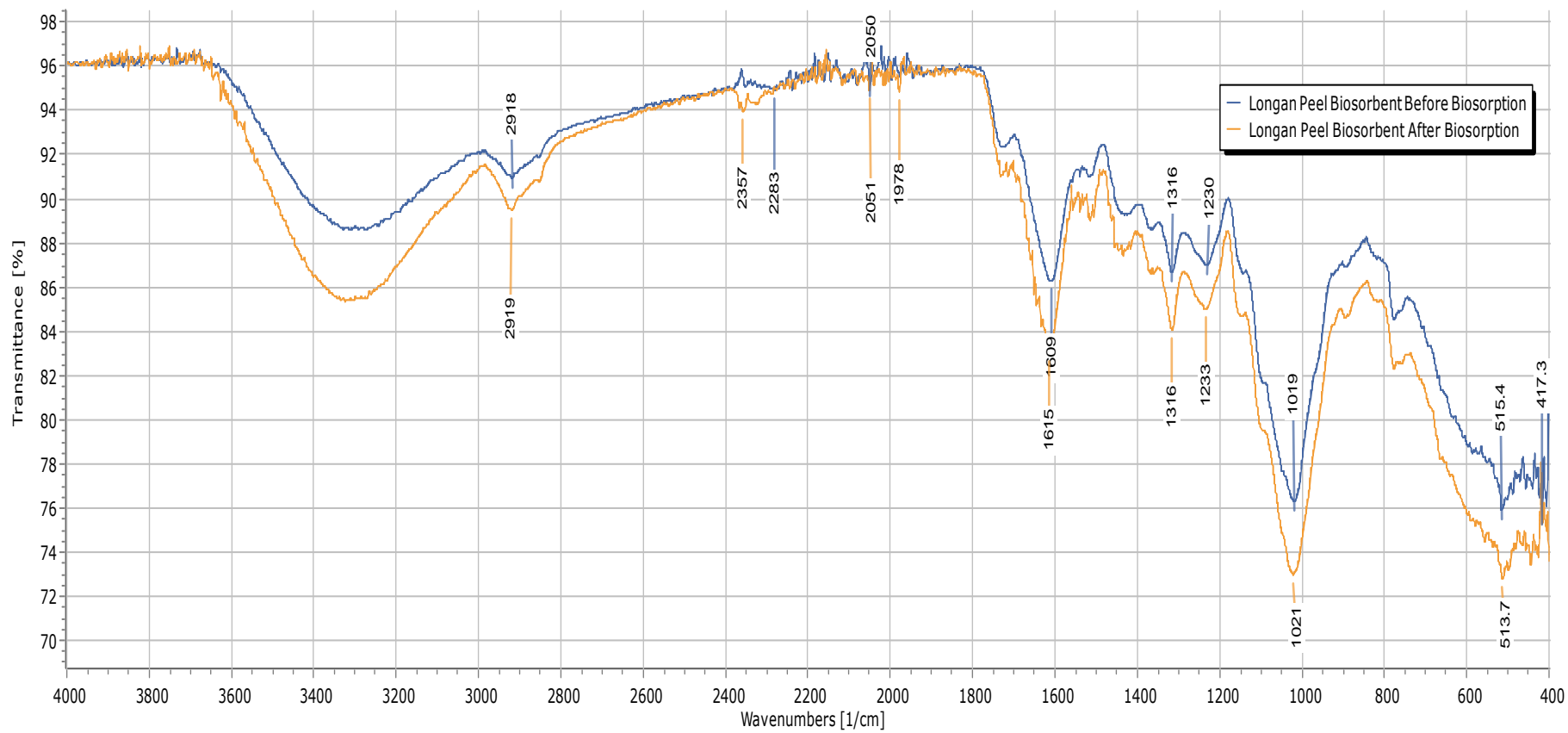
Figure 4.1: Stacked FTIR Spectra of Longan Peel Biosorbent Before and After Biosorption

4.1.2 FTIR Spectra of Activated Carbon

In both the spectra before and after adsorption by activated carbon shown in Figure 4.2, the presence of noise is observed for wavenumbers in the range of 4000 cm^{-1} to 3400 cm^{-1}. The noise can be attributed to the water vapour absorption from the atmosphere (Shimadzu Corporation, 2020). Therefore, the peaks in this region are ignored from the analysis of the spectra.

Before adsorption, the bands observed at 2993 and 2897 cm^{-1} indicate the existence of asymmetric and symmetric stretching by methylene groups respectively that are associated with aliphatic compounds (Bouhamed et al., 2014). However, these peaks were not present after the adsorption of Ni (II). The bands at 1561 to 1460 cm^{-1} can be attributed to asymmetric C–H aliphatic bending (Cuhadaroglu and Uygun, 2008).

Besides, a series of weak peaks centered on 1063 cm^{-1} indicates the presence of –CO bonds associated with organic acids, ether, esters, and phenols (Alcaraz et al., 2018). The disappearances of these peaks in the spectra after adsorption suggests that the aforementioned functional groups play some role in the adsorption of nickel ions from the solution.

After adsorption, there is a presence of a strong and wide peak at the 3400 cm^{-1} to 3000 cm^{-1} region, indicating –OH stretching of the hydroxyl functional group and possible chemisorption of water. The asymmetry of this particular band at a lower wavenumber region of 1200 cm^{-1} to 1000 cm^{-1} hints at the existence of strong hydrogen bonds (Dantas et al., 2010). The significant shift of the entire spectra to lower transmittance values after adsorption is a possible indicator that weak or broken absorption bands such as the –OH and –CO due to nickel ions bonding with the carbonyl groups could not be illustrated by the spectrum (Moyo et al., 2016). Table 4.2 summarises the functional groups associated with the peaks that were present in the activated carbon FTIR spectra before and after nickel adsorption took place.

Table 4.2: Principal Bands Ascribed to Activated Carbon Before and After Nickel Adsorption

Wavelength/ cm^{-1}	Functional group	Before adsorption	After adsorption
3400 - 3000	–OH stretching		✓
2993	Asymmetric C–H stretching	✓	
2897	Symmetric C–H stretching	✓	
1561 - 1460	Asymmetric C–H bending	✓	✓
1200 - 1000	–OH stretching		✓
1063	CO bonds	✓	
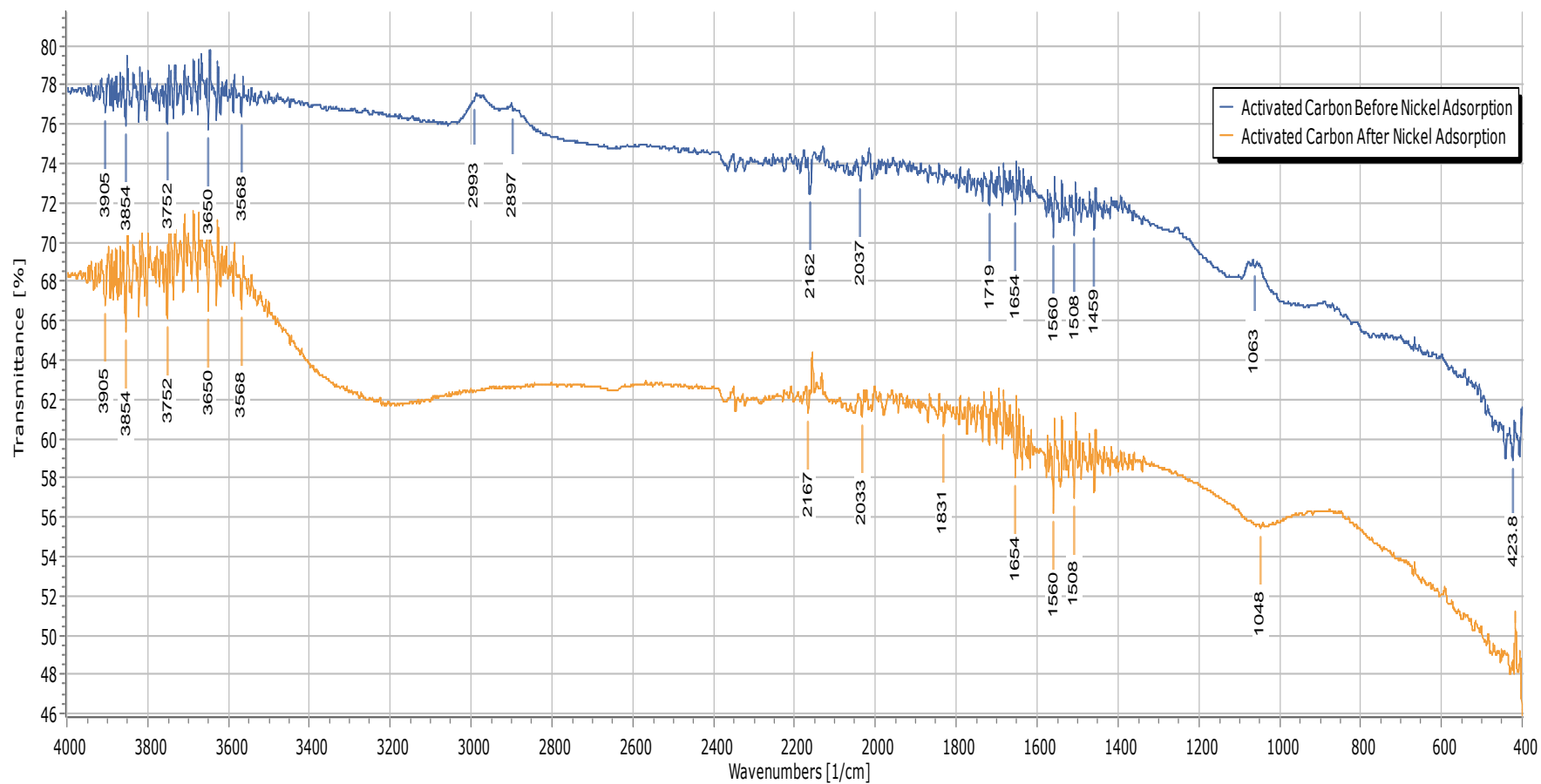
Figure 4.2: Stacked FTIR Spectra of Activated Carbon Before and After Nickel Adsorption

4.2   Modelling of Responses

4.2.1   Insertion of Data into Design Matrix

The three-factor, three-level Box-Behnken design combined with response surface modelling was chosen as a means to investigate the influence that the three independent variables, namely initial nickel concentration (*A*), adsorbent dosage (*B*), and pH (*C*) have on the removal efficiency of the nickel ions. Table 4.3 compares the adsorption uptake and removal efficiencies of longan peels and activated carbon at the experimental conditions set by the Box-Behnken design.

Runs 2, 3, 9, 11, and 15 constitute the five center points in the design matrix that are used to detect the presence of a possible curvature in the response. From Table 4.3, it is observed that the nickel adsorption uptake and removal efficiencies at these center points for both adsorbents are close to each other which indicates that the experimental data consists of replicable results.

The adsorption uptake and removal efficiency by activated carbon are higher than longan peel biosorbent for all the experimental runs except Run 8. As activated carbon has been established as a well-known adsorbent used in wastewater treatment, its higher performance in the nickel ions adsorption from the prepared solutions compared to a novel biosorbent sourced from longan waste peels was expected. The primary hypothesised reason for the high removal efficiency by activated carbon is due to its much larger internal surface area that was generated through a process of activation. Its Brunauer, Emmett and Teller (BET) surface area typically ranges between 500 to 1500 m^2/g while longan peel powder is reported by Chowdhury et al. (2018) to only have a BET surface area of 3.02 m^2/g. Besides its large surface area, its microporous ability and the chemical complexity of its external area greatly enhances its adsorption capabilities (Ahmad and Azam, 2019).

It was determined after a trial-and-error process that it is more suitable to perform model fitting based on the response of removal efficiencies rather than the adsorption uptakes.

Table 4.3: Adsorption Uptake and Removal Efficiencies of Longan Peel Biosorbent (Longan) and Activated Carbon (AC)

Run	A		B		C		Adsorption Uptake (mg/g)		Removal Efficiency (%)	
	Coded	Actual	Coded	Actual	Coded	Actual	Longan	AC	Longan	AC
1	-1.000	10.00	1.000	10.00	0.000	5.000	0.05050	0.08350	36.59	93.19
2	0.000	155.0	0.000	5.500	0.000	5.000	1.090	1.522	37.82	56.04
3	0.000	155.0	0.000	5.500	0.000	5.000	1.024	1.483	35.88	54.58
4	1.000	300.0	0.000	5.500	-1.000	2.000	1.269	2.265	27.20	41.71
5	0.000	155.0	-1.000	1.000	1.000	8.000	2.930	4.660	20.10	29.64
6	0.000	155.0	1.000	10.00	-1.000	2.000	0.5279	0.9230	37.63	71.11
7	0.000	155.0	-1.000	1.000	-1.000	2.000	0.8300	3.743	7.192	23.23
8	1.000	300.0	-1.000	1.000	0.000	5.000	8.020	6.860	26.69	23.07
9	0.000	155.0	0.000	5.500	0.000	5.000	0.7718	1.513	37.04	55.69
10	1.000	300.0	0.000	5.500	1.000	8.000	1.118	1.671	26.86	40.50
11	0.000	155.0	0.000	5.500	0.000	5.000	1.059	1.607	39.84	59.16
12	-1.000	10.00	-1.000	1.000	0.000	5.000	0.5390	0.6570	38.47	60.72
13	1.000	300.0	1.000	10.00	0.000	5.000	1.301	2.048	43.31	63.11
14	-1.000	10.00	0.000	5.500	1.000	8.000	0.09873	0.1602	37.37	93.92
15	0.000	155.0	0.000	5.500	0.000	5.000	1.265	1.345	39.21	54.69
16	0.000	155.0	1.000	10.00	1.000	8.000	0.4020	0.9371	39.49	74.26
17	-1.000	10.00	0.000	5.500	-1.000	2.000	0.03891	0.1633	25.36	86.43

4.2.2 Fitting of Model and ANOVA

The removal efficiency values for longan peel and activated carbon were both fitted to reduced cubic models. Analysis of variance (ANOVA) as shown in Table 4.4 and Table 4.5 were performed on the longan peel and activated carbon models respectively. Furthermore, the significance of each of the models was evaluated using lack-of-fit tests.

Table 4.4: ANOVA and Fit Statistics Results for Longan Peel Model

Source	Sum of Squares	df	Mean Square	F-value	p-value	Characteristics
Model	1352.67	10	135.27	61.89	< 0.0001	Significant
A	23.59	1	23.59	10.79	0.0167	Significant
B	620.69	1	620.69	284.01	< 0.0001	Significant
C	87.36	1	87.36	39.97	0.0007	Significant
AB	85.55	1	85.55	39.14	0.0008	Significant
AC	38.20	1	38.20	17.48	0.0058	Significant
BC	30.48	1	30.48	13.94	0.0097	Significant
A^2	2.07	1	2.07	0.9462	0.3683	Not significant
B^2	24.14	1	24.14	11.04	0.0159	Significant
C^2	377.15	1	377.15	172.57	< 0.0001	Significant
A^2B	153.87	1	153.87	70.41	0.0002	Significant
Residual	13.11	6	2.19			
Lack of Fit	2.82	2	1.41	0.5476	0.6163	Not significant
Fit Statistics						
R^2				0.9904		
Adjusted R^2				0.9744		
Predicted R^2				0.9057		
Adequate Precision				29.6673		

Table 4.5: ANOVA and Fit Statistics Results for Activated Carbon Model

Source	Sum of Squares	df	Mean Square	F-value	p-value	Characteristics
Model	7626.87	10	762.69	286.71	< 0.0001	Significant
A	2407.67	1	2407.67	905.09	< 0.0001	Significant
B	2138.65	1	2138.65	803.96	< 0.0001	Significant
C	31.37	1	31.37	11.79	0.0139	Significant
AB	14.32	1	14.32	5.38	0.0595	Slightly significant
AC	18.95	1	18.95	7.12	0.0371	Significant
BC	2.67	1	2.67	1.00	0.3551	Not significant
A^2	423.51	1	423.51	159.20	< 0.0001	Significant
B^2	155.44	1	155.44	58.43	0.0003	Significant
A^2B	49.91	1	49.91	18.76	0.0049	Significant
AB^2	115.60	1	115.60	43.45	0.0006	Significant
Residual	15.96	6	2.66			
Lack of Fit	2.11	2	1.06	0.3052	0.7528	Not significant
Fit Statistics						
R^2						0.9979
Adjusted R^2						0.9944
Predicted R^2						0.9850
Adequate Precision						54.6573

As demonstrated in Table 4.4 and Table 4.5, the longan peel and activated carbon models which have *F*-values which are 61.89 and 286.71 respectively, also have *p*-values that are less than 0.05. This verifies that both the models are significant. From Table 4.4, the initial nickel concentration, adsorbent dosage, and pH terms (*A*, *B*, and *C*), as well as the interaction effects shown by the *AB*, *AC*, *BC*, B^2, C^2, A^2B terms of the longan peel model, are significant as they have *p*-values which are less than 0.05 while the A^2 term is insignificant as its *p*-value is larger than 0.1. Based on the same reasoning, the *A*, *B*, *C*, *AC*, A^2, B^2, A^2B, AB^2 produce appreciable effects on the removal efficiency of activated carbon while the *BC* term does not.

The test for lack-of-fit of the longan peel model shows an *F*-value of 0.5476 that is insignificant as its *p*-value is 0.6163 which is more than 0.05. The same can be

said for the activated carbon model which its lack of fit test showed an F-value of 0.3052 with a p-value of 0.7528. Both the models are valid to be analysed further as they showed non-significant lack-of-fit.

The adequate precision for the longan peel and activated carbon model are 29.6673 and 54.6573 respectively. As both these values are greater than four, this is an indication that the models have strong enough signals for optimisation to be carried out.

4.2.3   Model Equations

Equation 4.1 and Equation 4.2 in terms of coded values model the removal efficiency by longan and activated carbon respectively. These equations demonstrate the effects of the three parameters as well as their interactions with each other on the response.

$$Removal\ Efficiency\ of\ Longan\ Peel\ (\%) = 37.9595 - 1.7172A + 12.4568B + 3.30448C + 4.6246AB - 3.09037AC - 2.76024BC + 0.700805A^2 - 2.39421B^2 - 9.46429C^2 - 8.77139A^2B \qquad (4.1)$$

$$Removal\ Efficiency\ of\ Activated\ Carbon\ (\%) = 55.8521 - 24.534A + 23.1228B + 1.98027C + 1.89177AB - 2.17641AC - 0.817081BC + 10.015A^2 - 6.06754B^2 - 4.99547A^2B + 7.60249AB^2 \qquad (4.2)$$

The terms with a positive sign indicate a synergistic impact on the response while an antagonistic impact is represented by terms with a negative sign (Alkhatib, Muyibi and Amode, 2011). Therefore, as adsorbent dosage and pH rises, the removal efficiency by longan peel and activated carbon is expected to also increase. On the contrary, the removal efficiencies of both adsorbents are predicted to drop as the initial nickel concentration increases. The explanation of the behaviour of the adsorption process due to the parameters will go into further detail in Section 4.3.

The R^2 value or the coefficient of determination is another indication of the degree of fit of the data. An R^2 value of at least 0.8 shows an acceptable goodness of fit for the model (Joglekar and May, 1987). Table 4.4 and Table 4.5 show the R^2, the adjusted R^2, and the predicted R^2 values for the longan peel and activated carbon models. Based on the tabulated values which are well over 0.8, the studied response model can be used to explain the adsorption results accurately.

4.2.4   Model Accuracy Check

4.2.4.1   Plots of Predicted versus Actual Results

The precision of the model can be assessed by comparing the actual removal efficiencies determined experimentally with the predicted results generated by the model.   Figure 4.3 (a) and (b) demonstrate the linear relationship between the predicted and actual removal efficiencies by longan peel and activated carbon respectively. As highlighted in Table 4.4 and Table 4.5, the predicted R^2 values for both models are close to the R^2 value which means that the removal efficiencies determined experimentally are well in line with values that were predicted with the model equation.
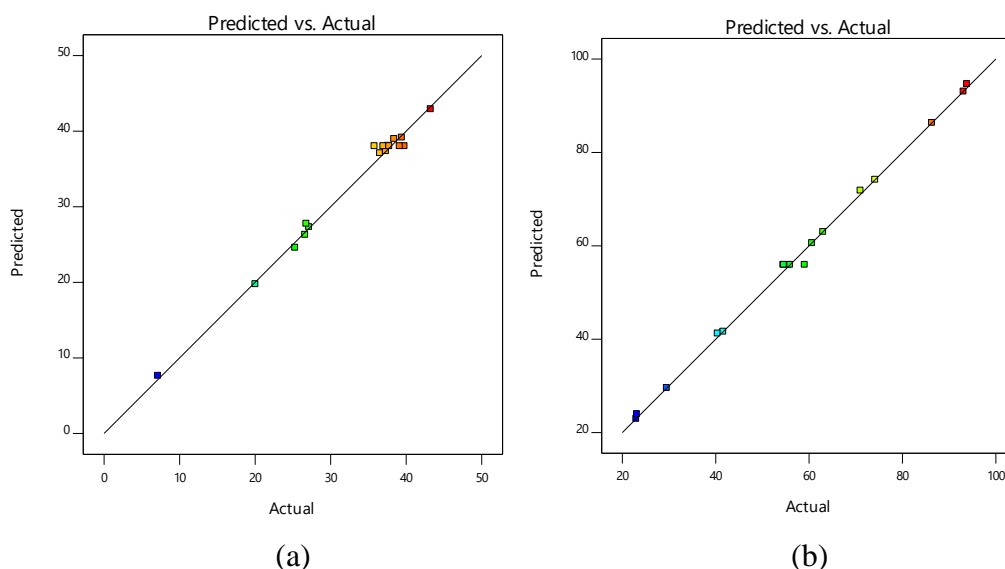
Figure 4.3: Plot of Predicted versus Actual Removal Efficiencies of a) Longan Peels
b) Activated Carbon

The difference between actual and predicted results may have been attributed to the common experimental errors that take place during the conducting of the experiments such as parallax error when reading the measurement graduations on instruments like the measuring cylinders and volumetric flasks. Besides, random errors also occur due to fluctuation in the readings of the pH meter and analytical balance. These two sources of errors may have resulted in the creation of inaccurate conditions for the experiments to take place. Furthermore, control experiments such as blanks with adsorbents and solutions which are adsorbent-free under the same experimental conditions were not conducted to determine if glassware sorption or if

metal precipitation takes place. In addition, only the initial pH was adjusted for each run while the more accurate step would be to constantly maintain the pH of the solution at a certain value through the addition of buffer solutions or acid/alkalis during the entirety of the adsorption experiment (Park, Yun and Park, 2010).

4.2.4.2 Normal Probability Plot of Residuals

Figure 4.4 (a) and (b) represent the normal plot of residuals for the longan peel and the activated carbon models respectively where normal probability is plotted against internally studentized residuals. These plots show that response transformations were not necessary as the criteria of assuming normality was met due to the approximation of the plots along the plotted straight lines.
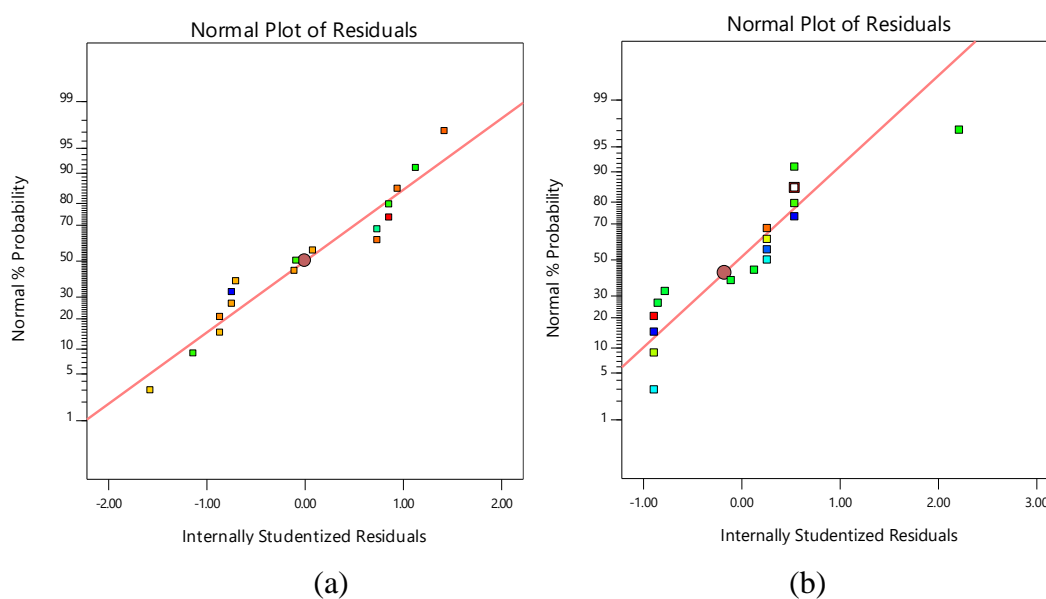
Figure 4.4: Normal Probability Plot of Residuals for the a) Longan Peel Model b) Activated Carbon Model

Residuals versus the predicted removal efficiency values by longan peel and activated carbon were plotted in Figure 4.5 (a) and (b) respectively. The plotted points are a random scatter which is another indication that response values from both models do not require any transformation (Stat-Ease Inc., 2020).
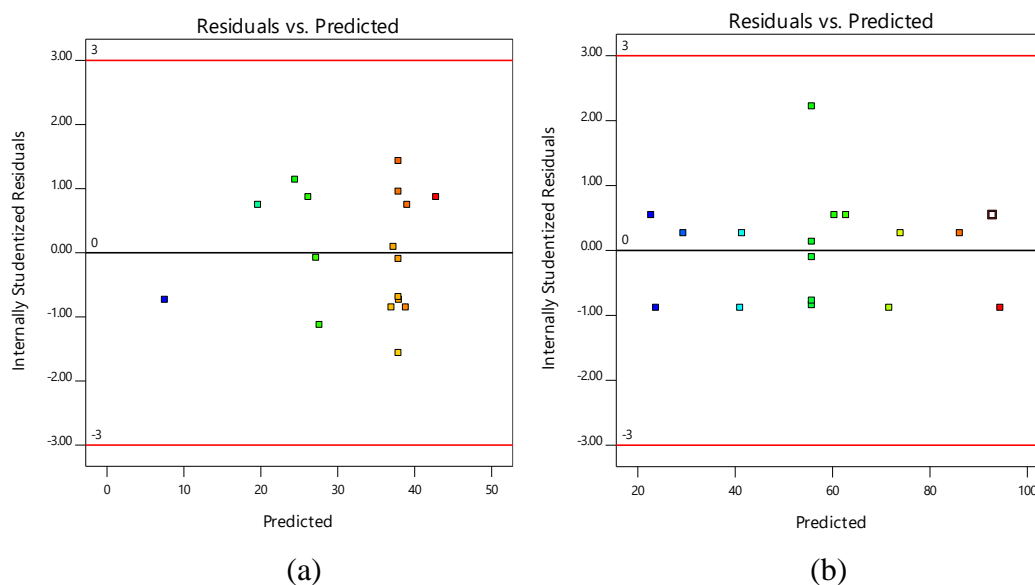
Figure 4.5: Plot of Residuals versus Predicted Removal Efficiencies by a) Longan Peel b) Activated Carbon

4.3 Results Analysis via Response Surface Methodology

The extent to which each of the parameters affects the removal efficiencies can be determined through perturbation plots. By default, the middle points of design space which are coded as zero levels (initial nickel concentration of 155 mg/L, adsorbent dosage of 5.5 g, and pH 5) were set as the reference points for each of the factors (Stat-Ease Inc., 2020).

To study the interacting effects between the three parameters, the response surface plots of removal efficiencies of the adsorbents versus the significant variables for each pair of factors at the center point of the remaining factor were plotted. The interacting effects that exist between the variables can be evaluated based on the curvature of the plots (Bagheri et al., 2019).

By utilizing the "Optimization" feature on Design Expert, the experimental results were optimised using a desirability function approach to recommend the optimal conditions for each adsorbent. To validate the optimisation results, the optimum conditions were recreated in the laboratory and the batch adsorption tests were conducted.

4.3.1 Longan Peel Biosorbent

4.3.1.1 Single Factor Analysis

As depicted in Figure 4.6, the removal efficiency of longan peels was observed to decrease steadily with a rise in initial nickel concentration. On the contrary, an upward trend for removal efficiency is depicted by the perturbation plot when the longan peel biosorbent dosage increases. An increase in removal efficiency was a result of the pH increase up to a certain point and then the efficiency drops beyond that point.
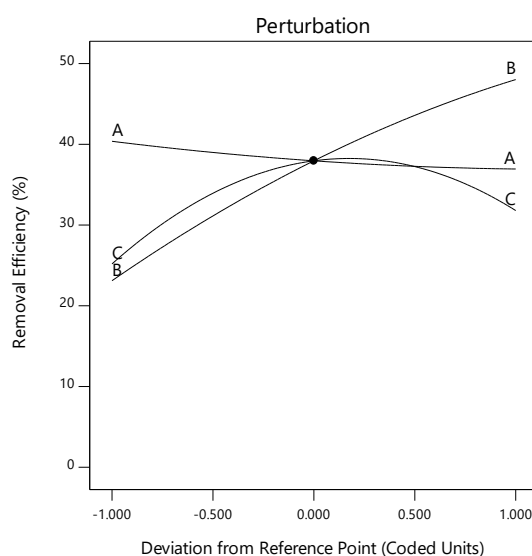
Figure 4.6: Perturbation Plot of Initial Nickel Concentration, Biosorbent Dosage, pH for Longan Peel Biosorbent Model.

4.3.1.2 Interaction between Initial Nickel Concentration and Biosorbent Dosage

Figure 4.7 shows the interacting effects between initial nickel concentration and the biosorbent dosage in removing nickel ions from the aqueous solutions at a pH of 5. Based on the interacting effects between these two parameters, the maximum removal efficiency is 48.28 % at an initial nickel concentration of 181.1 mg/L with 10 g of longan peel biosorbent dosage.

At any initial nickel concentration, the removal efficiency shows an increasing trend when the longan peel biosorbent dosage increases. This is supported by the fact that increasing the dosage of the biosorbent means that there is more surface area available for the nickel ion to be adsorbed. By the same token, increasing the initial nickel concentration does not yield higher removal efficiencies

unless it is accompanied by a higher amount of biosorbent dosage. This can be explained by the excess of nickel ions in the bulk fluid in comparison to the number of active sites present on the surface of the biosorbent (Biswas et al., 2019).

Figure 4.7: Effect of Initial Nickel Concentration and Longan Peel Biosorbent Dosage on Removal Efficiency (a) 3D response surface and (b) contour plot of the predicted removal efficiency.

4.3.1.3 Interaction between Initial Nickel Concentration and pH

Figure 4.8 shows the interacting effects between initial nickel concentration and the pH of the aqueous solution when the biosorbent dosage has been fixed at a center point of 5.5 g. The maximum removal efficiency of 41.46 % is achieved when the aqueous solution has an initial nickel concentration of 10 mg/L and pH of 6.031.

At all initial nickel concentrations, the removal efficiency of longan peels was observed to increase when the pH increases from an acidic pH 2.00 to the slightly acidic range of pH 5.00 to 6.00. At lower pH values, the active sites present on the surface of the biosorbent may become protonated which causes electrostatic repulsion between the positive charges of the ligand on the surfaces of the longan peel and nickel cations. There is also competition between the nickel ions and the protons (H^+ and H_3O^+ ions) to occupy the available adsorption sites (Ouyang et al., 2019). By increasing in the pH of the solution, the surface charge of the longan peel biosorbent becomes more negative. Consequently, there will be less electrostatic repulsions that exist between the nickel cations and the negatively-charged surface of the biosorbent as well as less competition between the protons and cations for the

same functional groups (Guo et al., 2018). However, the removal efficiency values start to decrease when the solution pH is either neutral or slightly basic. This is due to the simultaneous occurrence of the formation of insoluble nickel hydroxides and the biosorption of nickel with the former being favoured over the latter (Guo et al., 2018).
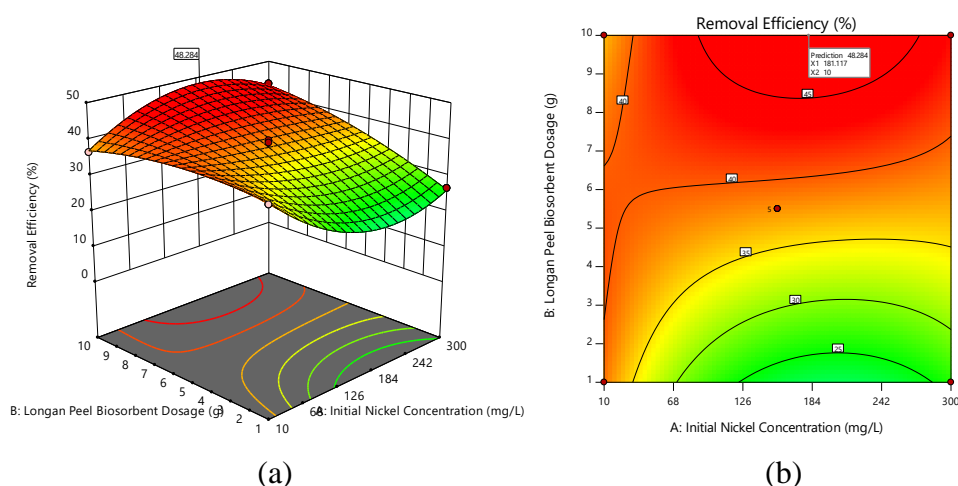

| (a) | (b) |
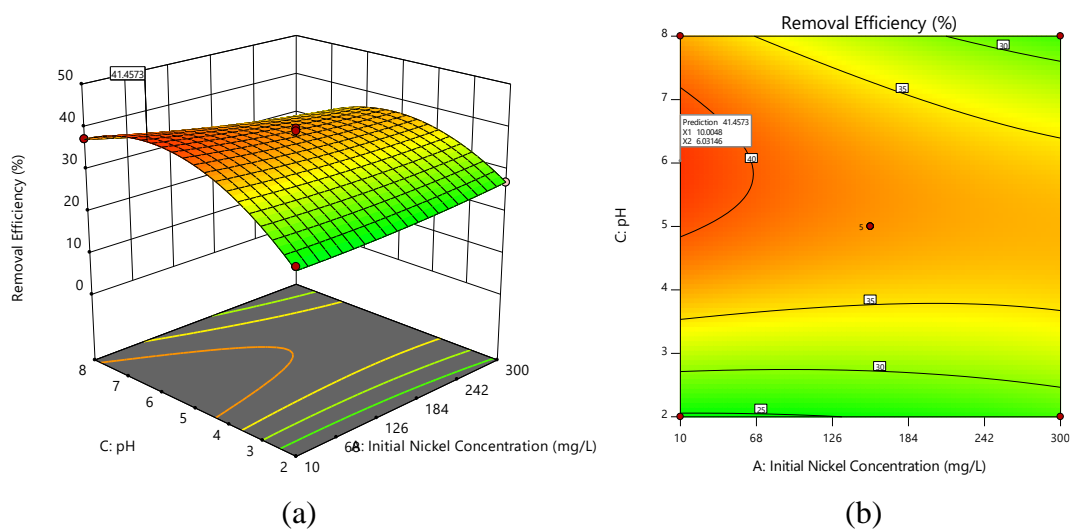
Figure 4.8: Effect of Initial Nickel Concentration and pH of Solution on Removal Efficiency (a) 3D Response Surface and (b) Contour Plot of the Predicted Removal Efficiency by Longan Peel Biosorbent.

4.3.1.4 Interaction between Biosorbent Dosage and pH

Based on Figure 4.9, when the initial nickel concentration is fixed at a center point of 155 mg/L, increased removal efficiencies are achieved when the longan peel biosorbent dosage is at its highest and when the pH is in the slightly acidic range of pH 5.00 to 6.00. More specifically, the maximum removal efficiency is 48.03 % when the biosorbent dosage is 10.00 g and the pH is 5.080. As highlighted previously, the increased dosage means more active sites for biosorption to take place whereas the slightly acidic pH range results in a more negative surface charge to facilitate in the biosorption of the positive nickel ions onto the surface.
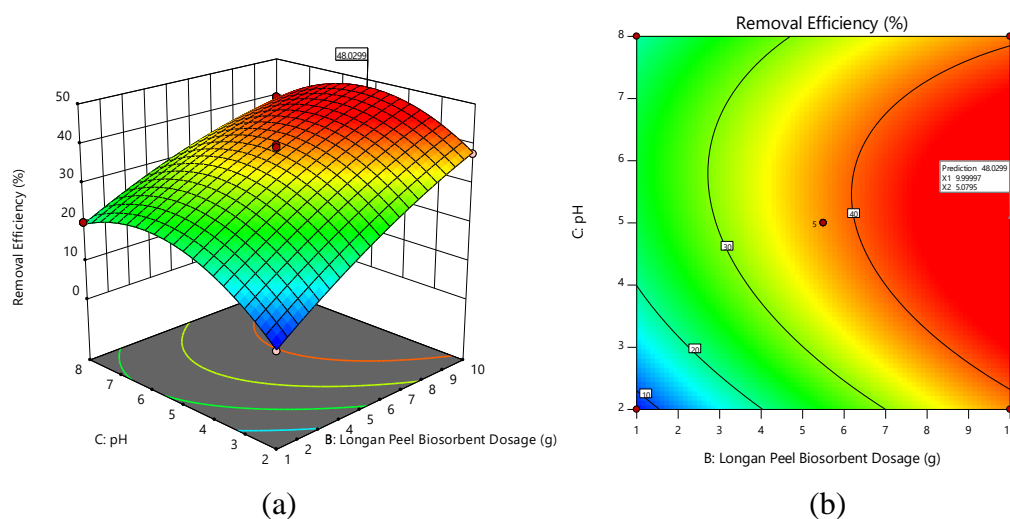
Figure 4.9: Effect of Longan Peel Biosorbent Dosage and pH on Removal Efficiency (a) 3D Response Surface and (b) Contour Plot of the Predicted Removal Efficiency.

4.3.1.5 Optimisation

The removal efficiency of longan peel predicted at optimal conditions which is 47.64 % is tabulated along with the actual removal efficiency achieved experimentally in Table 4.6. There was a discrepancy of 4.658 % between the predicted and actual removal efficiency. As the values are within the acceptable margin of error, this serves as another indicator that the predicted and experimental values are in agreement, further proving that the longan peel biosorbent model is valid.

Table 4.6: Optimum Conditions for Biosorption and The Percentage Difference between Actual and Maximum Removal Efficiencies by Longan Peel Biosorbent

Initial Nickel Concentration (mg/L)	Biosorbent Dosage (g)	pH	Maximum Removal Efficiency (%)	Actual Removal Efficiency (%)	% Difference
180.17	9.708	5.346	47.64	45.42	4.658

4.3.2   Activated Carbon

4.3.2.1   Single Factor Analysis

According to Figure 4.10, the initial nickel concentration has an inverse relationship with removal efficiency. Similar to the trend observed for the longan biosorbent dosage, when the activated carbon dosage increases, the removal efficiency increased sharply. An upward trend is also illustrated by the perturbation plot of the pH factor. However, the effect of pH is much smaller in comparison with the effect of adsorbent dosage.
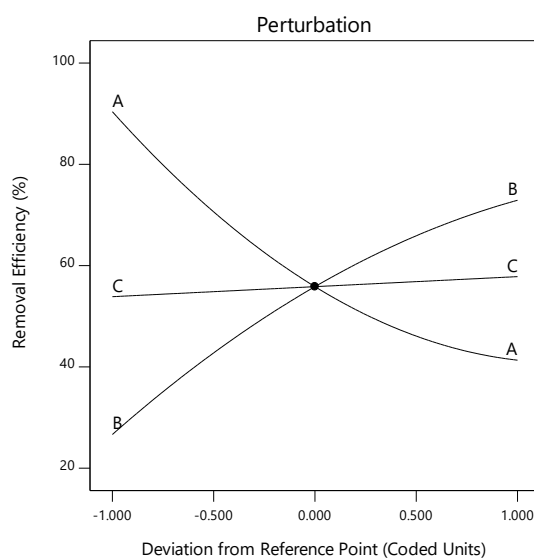
Figure 4.10: Perturbation Plot of Initial Nickel Concentration, Adsorbent Dosage, pH for Activated Carbon Model

4.3.2.2   Interaction between Initial Nickel Concentration and Adsorbent Dosage

Based on Figure 4.11, the highest removal efficiency of 95.22 % is determined to be at a nickel ion concentration of 10.00 mg/L and adsorbent dosage of 8.187 g. By increasing the dosage of the activated carbon, higher removal efficiencies were observed across all initial nickel concentrations. The higher adsorbent dosages yield a large availability of surface area and active sites to increase the efficiency of adsorbing nickel cations present in the aqueous solution. When the dosage of activated carbon is low, there is a higher ratio of the nickel ions in comparison with the vacant sites available on the activated carbon surface. As a result, the removal efficiency is lowered.

There is a small region in the lower range of initial nickel concentrations where increasing the adsorbent dosage beyond a certain point results in lower removal efficiencies. This could be due to the adsorption sites that remain unsaturated as their number exceeds the number of nickel ions present in the low concentration bulk solution (Javanbakht and Ghoreishi, 2017). Consequently, the total surface area of the adsorbent is smaller and the path length for diffusion is longer (Shukla et al., 2002).

On the other hand, the removal efficiency decreases at larger initial nickel concentrations due to adsorption sites being saturated with the nickel ions. With lower concentrations, the ratio of the nickel ions to the adsorption sites is lower resulting in higher removal efficiencies.

(a) (b)

Figure 4.11: Effect of Initial Nickel Concentration and Activated Carbon Dosage on Removal Efficiency (a) 3D Response Surface and (b) Contour Plot of the Predicted Removal Efficiency.

4.3.2.3 Interaction between Initial Nickel Concentration and pH

From Figure 4.12, an increasing trend in the removal efficiency is apparent when the pH increases from 2 to 8 at lower initial nickel concentrations. This may be a result of the functional groups on the activated carbon surface being protonated at lower pH values, resulting in a surface positive charge. This will result in the existence of significant repulsive forces between the nickel ions and the activated carbon that prevent adsorption from taking place efficiently. At higher pH values, the adsorption sites which are the OH and COOH functional groups are deprotonated which allow

hydrogen bonding and/or electrostatic interaction to be involved as the removal mechanisms in the adsorption process (Bagheri et al., 2019).

At higher initial nickel concentrations, the removal efficiency is low and fluctuates between constant values despite an increase in pH of the solution. Similar to the experimental runs associated with the longan peel biosorbent, the low removal efficiencies may be attributed nickel ions in the bulk solution that are in excess of the active sites that are present on the adsorbent surface (Biswas et al., 2019). Taking both these parameters into account, the highest removal efficiency of 94.56 % is achieved at an initial nickel concentration of 10 mg/L and a solution pH of 8.00.
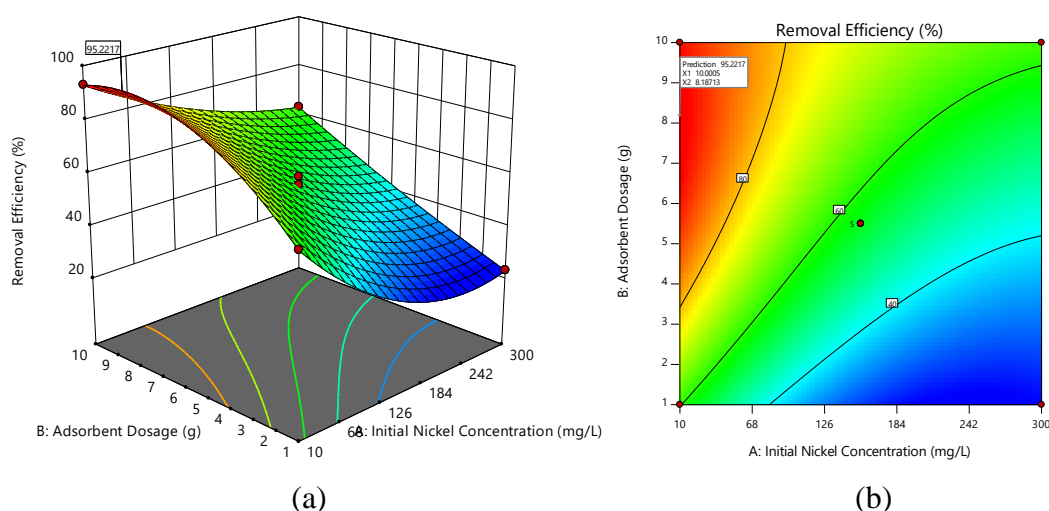

(a)   (b)
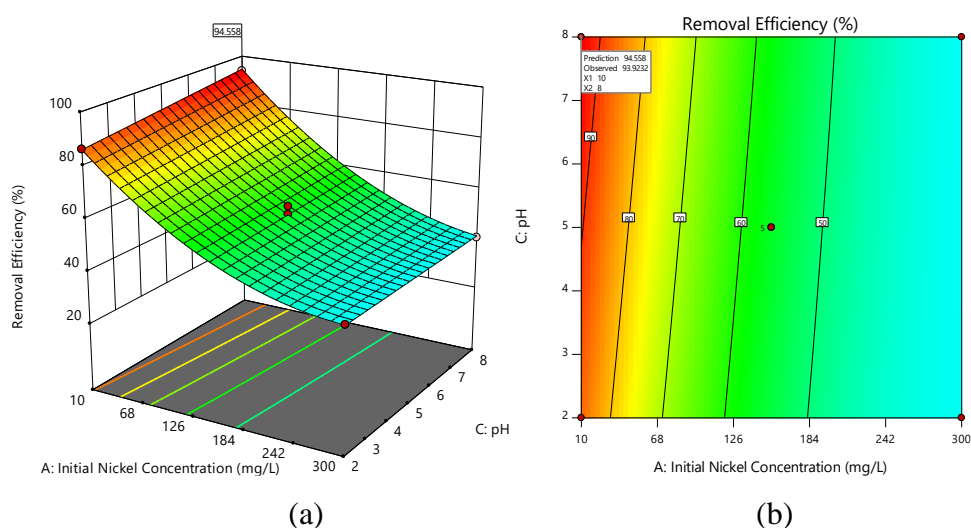
Figure 4.12: Effect of Initial Nickel Concentration and pH of Solution on Removal Efficiency (a) 3D Response Surface and (b) Contour Plot of the Predicted Removal Efficiency by Activated Carbon.

4.3.2.4 Interaction between Adsorbent Dosage and pH

Based on Figure 4.13, the removal efficiency increases with higher activated carbon dosages. The pH of the solution does not produce any noticeable effect on the removal efficiency for any amount of dosage. This suggests that the dosage of activated carbon has a more significant impact on the efficiency of activated carbon in removing nickel ions from the solution compared to pH. Overall, it is also evident that none of the interactions between these two parameters produce a removal efficiency that exceeds 75 %, which is well below the maximum that was achieved by the interacting effects between the other combination of terms. This corroborates

with the ANOVA results for the activated carbon model made in Table 4.5 that showed that the *BC* term is not significant.
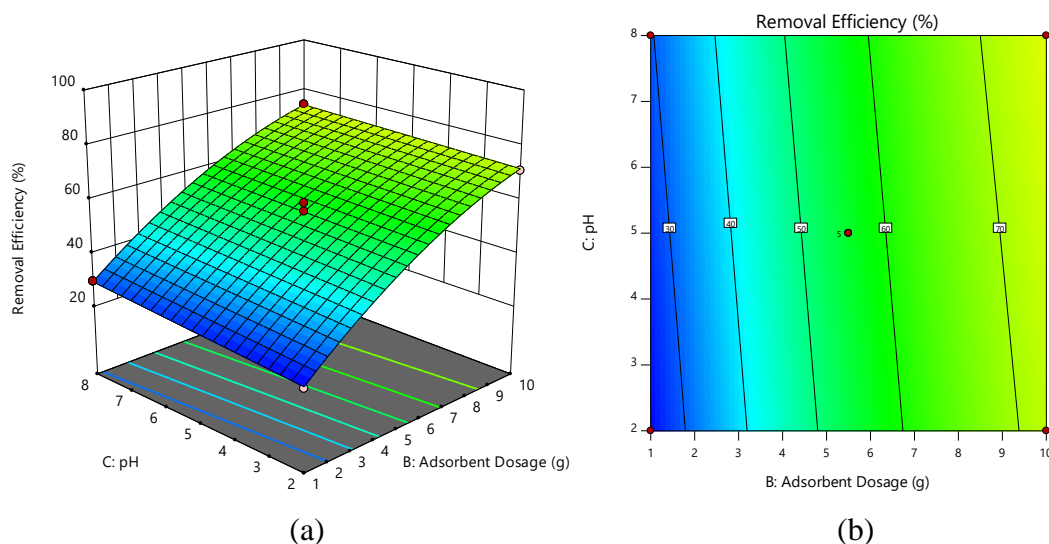
Figure 4.13: Effect of Activated Carbon Dosage and pH on Removal Efficiency (a) 3D Response Surface and (b) Contour Plot of the Predicted Removal Efficiency.

4.3.2.5 Optimisation

Optimisation of the parameters in the activated carbon model yields a maximum removal efficiency of activated carbon which is 97.85 %. The actual removal efficiency obtained through the recreation of the optimum conditions is shown in Table 4.7. There was only a slight difference of 1.079 % between the predicted and actual removal efficiency by activated carbon. The closeness of the two values is further proof that the activated carbon model is valid.

Table 4.7: Optimum Conditions for Adsorption and The Percentage Difference between Actual and Maximum Removal Efficiencies of Activated Carbon

Initial Nickel Concentration (mg/L)	Adsorbent Dosage (g)	pH	Optimal Removal Efficiency (%)	Actual Removal Efficiency (%)	% Difference
11.94	7.585	7.999	97.85	96.79	1.079

4.4   Adsorption Isotherm

The quantitative relationship between nickel concentration and the adsorption process was established by linear mathematical models proposed by Langmuir and Freundlich. The batch adsorption experiments to verify the adsorption isotherm relationship were conducted with a contact time of three hours, a stirring speed of 180 rpm, and at the optimal conditions specified in Table 4.6 and Table 4.7 for longan peel and activated carbon respectively.

4.4.1   Langmuir Isotherm

Figure 4.14 and Figure 4.15 depict the linear plots of Langmuir isotherm for longan peel biosorbent and activated carbon respectively.
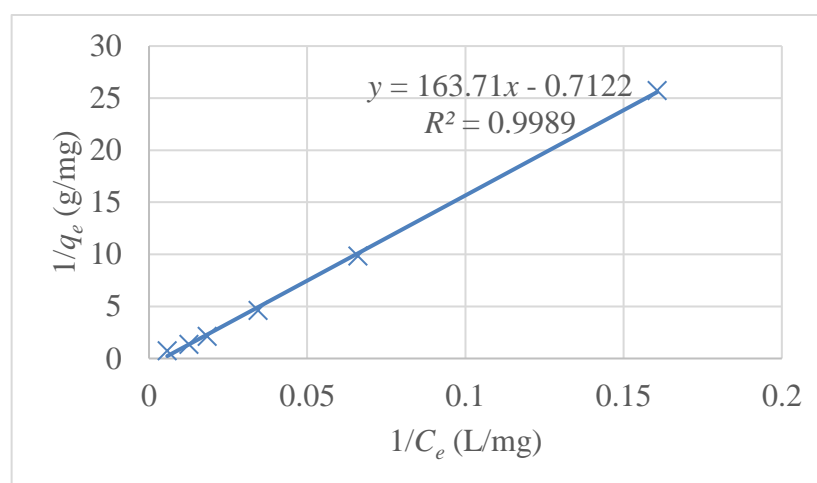
Figure 4.14: Plot of Langmuir Isotherm for Biosorption of Ni^{2+} by Longan Peel Biosorbent
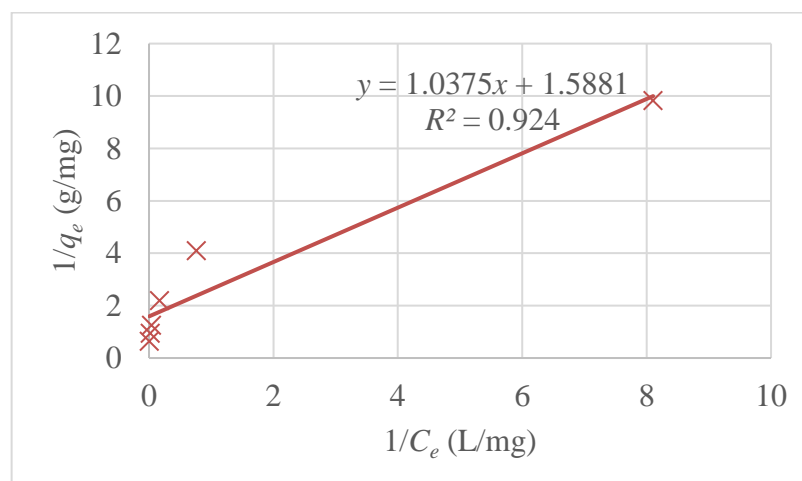
Figure 4.15: Plot of Langmuir Isotherm for Adsorption of Ni^{2+} by Activated Carbon

4.4.2 Freundlich Isotherm

Figure 4.16 and Figure 4.17 depict the linear plots of Langmuir isotherm for longan peel biosorbent and activated carbon respectively.
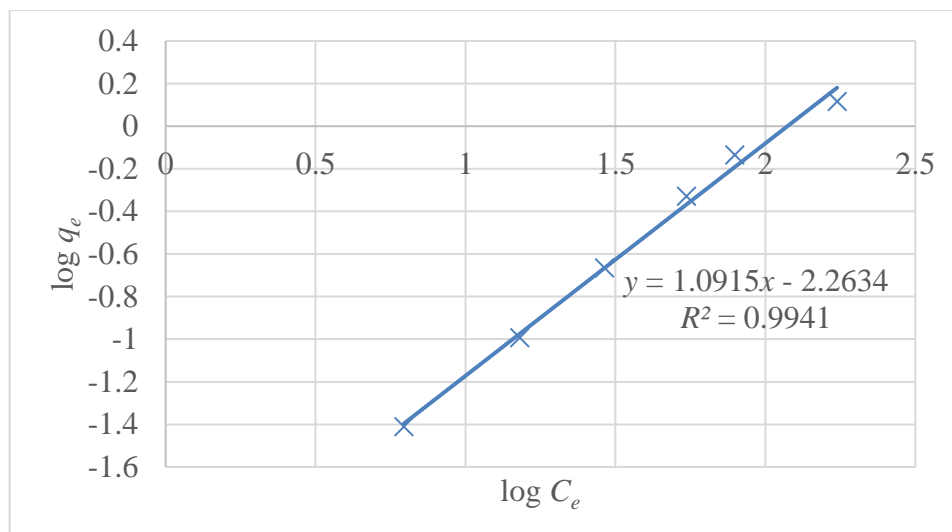
Figure 4.16: Freundlich Isotherm Plot for Biosorption of Ni^{2+} by Longan Peel Biosorbent
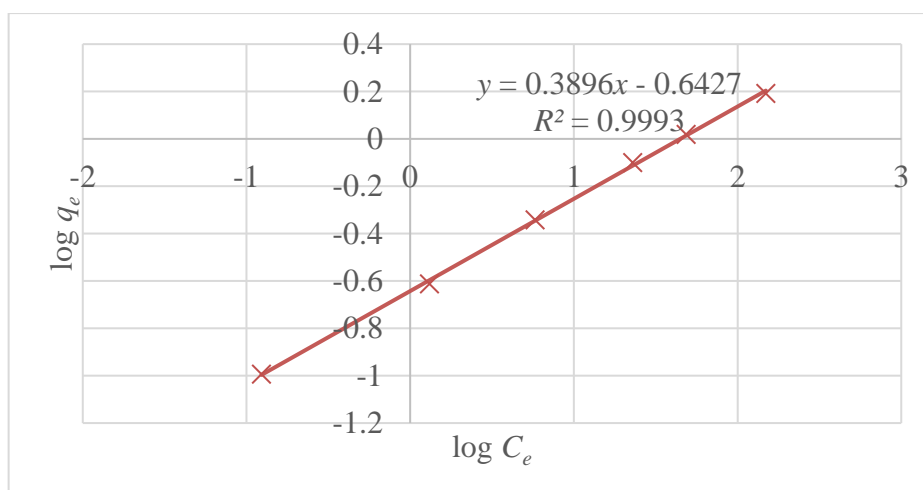
Figure 4.17: Freundlich Isotherm Plot for Adsorption of Ni^{2+} by Activated Carbon

4.4.3 Summary of Adsorption Isotherm Parameters

The relevant constants and correlation coefficient, R^2 of each model for both types of adsorbents are summarised Table 4.8. The equilibrium data for both the adsorbents were fitted well by both the Freundlich and Langmuir isotherm models as the R^2 values for all four plots are above 0.9. Nevertheless, the best fitting models for longan peel and activated carbon were Langmuir isotherm and Freundlich isotherm

respectively as they rendered the highest correlation coefficient values for each model. This means that biosorption by longan peel predominantly involves an ion exchange mechanism while the primary removal mechanism by activated carbon is through adsorption-complexation (Bulut and Tez, 2007).

The Freundlich intensity parameter, $1/n$ is more than 1 for the longan peel biosorbent (1.092) and less than 1 for activated carbon (0.3896). As stated by Ali et al. (2016), a value of $1/n$ which is below 1 is an indicator of normal adsorption whereas a value between 1 to 10 is a measure of favourable adsorption. This corroborates with the experimental results inputted into the design matrix as shown in Table 4.3 which shows that activated carbon had much higher removal efficiencies and nickel adsorption uptakes compared to the longan peel biosorbent.

The equilibrium data for adsorption by activated carbon was described slightly inadequate by Langmuir isotherm as evidenced by its lower R^2 value of 0.9240 whereas the longan peel fared better with an R^2 value of 0.9989. One of the assumptions for this isotherm was that all the active sites on the adsorbent surface should have equal affinities towards the nickel ions and adsorption is only confined to a monolayer surface. Another assumption is that the total quantity of active sites present on the adsorbent surface should not be exceeded by the number of adsorbate species. There is also the assumption of a finite number of identical binding sites and an absence of lateral interactive effects between the adsorbed species (Kowanga et al., 2016). It is theorised that none of these assumptions are applicable for activated carbon, thus explaining its lower R^2 value and therefore its supposedly smaller q_m value. Therefore, the Freundlich model which takes multilayer adsorption and surface roughness into consideration describes the equilibrium data of activated carbon adsorption better.

The maximum adsorption capacities, q_m of longan peel biosorbent and activated carbon were 1.404 and 0.6297 mg/g respectively which are significantly lower than the reported values of previously-studied biosorbents in Table 2.5. The current adsorption isotherm study involves 97.08 g/L of longan peel biosorbent dosage and 75.85 g/L of activated carbon dosage while the values tabulated in Table 2.5 were in the range of 0.6 to 8.2 g/L. As uptake rate has an inverse relationship with adsorbent dosage, the higher dosages used in the current study results in lower adsorption capacities.

Furthermore, the separation factor, R_L determined from the Langmuir model which gives insight into the nature of adsorption was also evaluated. The R_L values of longan peel and activated carbon were between 0 to 1 (0.9787 and 0.1151 respectively) which indicates a favourable adsorption process (Kowanga et al., 2016).

Table 4.8: Constant for Langmuir and Freundlich Isotherm for Ni adsorption by Longan Peel Biosorbent and Activated Carbon

Isotherm	Parameter	Adsorbent	
		Longan Peel Biosorbent	Activated Carbon
Langmuir	R^2	0.9989	0.9240
	K_L (L/mg)	4.350×10^{-3}	1.531
	q_m (mg/g)	1.404	0.6297
	R_L	0.9787	0.1155
Freundlich	R^2	0.9941	0.9993
	$1/n$	1.092	0.3896
	K_F	5.453×10^{-3}	0.2277

4.5 Feasibility of Longan Peel Biosorbent in Nickel Ion Removal from Wastewater

The longan peel is also assessed based on its suitability in being applied in the industrial scale.

4.5.1 Comparisons with Adsorbents

A side-by-side comparison of the performance of longan peels biosorbent with the other biosorbents that have been studied previously is necessary to determine the extent of its potential. Table 4.9 lists the maximum removal efficiency of the biosorbents achieved at optimum conditions reported in past studies as well as the longan peel and activated carbon studied in the current research. It is evident that longan peels have a much lower removal efficiency compared to the other tabulated biosorbents.

The lower performance of longan peels in the removal of nickel could be due to a lack of surface oxidation, surface treatment, or functionalization on the surface of this biosorbent. On the contrary, the watermelon rind was activated with zinc chloride and the plantain peels were modified using 5 % NaOH. Chemical activation

increases the number of binding sites that are accessible for interaction and allows for new functional groups formation, resulting in improvements with the adsorption capacity of the biosorbents (Oghenejoboh, 2018).

On the other hand, the cell walls of bacterial biosorbents like *Aspergillus niger* as well as algae such as *Hypnea valentiae* and *Enteromorpha* sp. consist of functional groups that include phosphonate, amino, hydroxyl, and carboxyl which are responsible for the nickel ions chemisorption. The phosphonate and amine groups were not detected by the longan peel FTIR spectrum in Figure 4.1 which may have contributed to the lower adsorption performance of longan peels.

4.5.2   Application in Wastewater Treatment Industry

The viability of using longan peel biosorbent as a substitute of powdered activated carbon dosed in aeration tanks for wastewater treatment such as the system shown in Figure 2.7 is also investigated. Based on the compilation of data from literature studies shown in Table 2.2, most industrial plants produce effluents with nickel concentrations between 1 to 300 mg/L. Depending on the location of wastewater discharge, the biosorption of nickel in wastewater would need to adhere to standards A and B set by Environmental Quality Regulations 2009 which are 0.20 mg/L and 1.0 mg/L respectively.

For the current system, the longan peel biosorbent was determined to adsorb a single adsorbate which is nickel most optimally at a pH of 5.436. However, industrial effluents consist of different concentrations of multiple coexisting metals at varying pH that can impair the performance of the biosorbent. Furthermore, the current laboratory study was conducted at an agitation speed of 180 rpm but the process is much more rapid in the industrial scale which could result in the surface of the biosorbent being saturated too quickly. Besides, wastewater treatment plants treat large cubic meters of water per day so contact times are often reduced to facilitate a fast and continuous treatment process. Therefore, the adsorption capacity of the longan peel biosorbent may be even lower in practice. Taking these factors into consideration, it is highly unlikely that biosorption by longan peel in its current form even with multiple biosorption cycles would be able to achieve standards A or B for industrial discharge.

Table 4.9: Optimum Conditions and Maximum Ni (II) Removal Efficiencies of Various Biosorbents

Biosorbent	Optimum Conditions			Maximum Ni (II) Removal Efficiency (%)	Reference
	Dosage (g)	Initial Nickel Concentration (mg/L)	pH		
Immobilized mixture of custard apple seeds and *Aspergillus niger*	10.00	100.0	5.60	96.41	(Saravanan, Senthil Kumar and Preetha, 2016)
Activated carbon from watermelon rind	5.000	100.0	6.69	97.00	(Oghenejoboh, 2018)
Modified plantain peel	0.820	120.0	4.36	94.88	(Garba, Ugbaga and Abdullahi, 2016)
Enteromorpha **sp.**	0.100	100.0	4.79	87.16	(Tolian, Jafari and Zarei, 2015)
Hypnea valentiae	1.275	100.0	5.10	91.97	(Shukla et al., 2002)
Regenerated cellulose	0.400	32.50	6.40	98.00	(Davarnejad, Moraveji and Havaie, 2018)
Saccharum bengalense **plant**	0.500	50.00	5.00	87.60	(Din and Mirza, 2013)
Aspergillus niger	0.2980	30.00	6.25	70.30	(Amini, Younesi and Bahramifar, 2009)
Longan peel	9.708	180.17	5.346	47.64	Present study
Commercial activated carbon	7.585	11.94	7.999	97.85	Present study

CHAPTER 5

CONCLUSIONS AND RECOMMENDATIONS

5.1 Conclusions

With the aid of Box-Behnken designs, three parameters which are initial nickel concentration, adsorbent dosage, and pH were optimised to maximise the nickel removal efficiency of two adsorbents namely, longan peel biosorbent and activated carbon. The effectiveness of using statistical design of experiments and RSM to study the interacting effects of the parameters is validated by the good agreement between the experimental and predicted values as well as the statistically significant models and insignificant lack-of-fit tests obtained from the ANOVA results.

Based on to the perturbation plots, it was determined that the removal efficiency of longan peel biosorbent and activated carbon decreases as the initial nickel concentration increases. Upward trends of removal efficiencies were observed for both types of adsorbents when the adsorbent dosages increase. The highest removal efficiencies of longan peel biosorbent were obtained when the pH is slightly acidic whereas basic pH range enhances the removal efficiency of activated carbon.

Based on optimisation by the desirability function approach, the maximum removal efficiency of longan peel is 47.64 % when the initial nickel concentration is 180.17 mg/L, the biosorbent dosage is 9.708 g, and the pH is 5.346. In comparison, the activated carbon has a much higher maximum removal efficiency of 97.85 % with optimised initial nickel concentration, adsorbent dosage, and pH of 11.94 mg/L, 7.585 g, and 7.999 respectively.

The best fitted models based on the equilibrium data obtained for longan peel biosorbent and activated carbon were determined to be the Langmuir isotherm and Freundlich isotherm model respectively.

Longan peel biosorbent did not achieve as high removal efficiencies as other reported biosorbents and commercial activated carbon. The lack of chemical activation or modification on the surface of the biosorbent and the absence of certain functional groups were the reasons cited for its underwhelming performance. The scale-up of the current longan peel biosorbent system cannot be readily applied in the actual wastewater treatment plant due to its inadequate removal efficiency as well as several field-based factors that may hinder its performance. Overall, the research

showed that there is potential for longan peel to be utilised as a biosorbent for the removal of nickel ions from aqueous solutions. However, there are several areas of improvement that can be explored to enhance the feasibility of adopting longan peel biosorption on an industrial scale.

5.2   Recommendations for Future Research

Several suggestions are proposed to improve the understanding of the biosorption mechanisms of longan peels in removing nickel contaminants. Besides, recommendations are made to help enhance the competitiveness of longan peel among the other low-cost biosorbents as well as increasing its potential as a possible replacement of activated carbon as an adsorbent in actual wastewater treatment plants. The recommendations are as follows:

(i)   Performance of kinetic studies to provide information on the rates of biosorbate uptake of the longan peel biosorbent and on the rate-controlling steps involved in biosorption such as intraparticle mass transfer, external mass transfer, and biosorptive reactions.

(ii)   Conducting surface area, porosimetry, particle size, hardness, and surface activity measurements to evaluate the characteristics of the longan peel surface that are crucial to the biosorption process.

(iii)   Chemical activation of the surface of the longan peel to increase the number of active sites available for biosorption.

(iv)   Performance of adsorption tests on industrial effluent which consists of coexisting pollutants including nickel to understand the potential of longan peel as a biosorbent for general purpose.

(v)   Conduct desorption studies to determine a suitable desorbing agent that can help both in the recovery of adsorbed nickel ions and in the regeneration of the longan peel biosorbent.

(vi)   Investigation of the adsorption performance of the longan peel biosorbent via a continuous mode of operation using an up-flow packed bed column reactor to better simulate the conditions of an actual wastewater treatment plant

REFERENCES

Abbas, S.H., Ismail, I.M., Mostafa, T.M. and Sulaymon, A., 2014. Biosorption of Heavy Metals: A Review. *Journal of Chemical Science and Technology*, 3, pp.74–102.

Ahmad, A. and Azam, T., 2019. 4 - Water Purification Technologies. In: A.M. Grumezescu and A.M.B.T.-B. and P.W. Holban, eds. [online] Woodhead Publishing, pp.83–120. Available at: <http://www.sciencedirect.com/science/article/pii/B9780128152720000040>.

Ahmaruzzaman, M., 2011. Industrial wastes as low-cost potential adsorbents for the treatment of wastewater laden with heavy metals. *Advances in Colloid and Interface Science*, [online] 166(1–2), pp.36–59. Available at: <http://dx.doi.org/10.1016/j.cis.2011.04.005>.

Akar, T., Kaynak, Z., Ulusoy, S., Yuvaci, D., Ozsari, G. and Akar, S.T., 2009. Enhanced biosorption of nickel(II) ions by silica-gel-immobilized waste biomass: Biosorption characteristics in batch and dynamic flow mode. *Journal of Hazardous Materials*, 163(2–3), pp.1134–1141.

Al-Duri, B., 1996. Adsorption modelling and mass transfer. In: G. McKay, ed., *The Use of Adsorbents for the Removal of Pollutants from Wastewater*, 1st ed. Boca Raton: CRC Press.

Alcaraz, L., López Fernández, A., García-Díaz, I. and López, F.A., 2018. Preparation and characterization of activated carbons from winemaking wastes and their adsorption of methylene blue. *Adsorption Science and Technology*, 36(5–6), pp.1331–1351.

Ali, M.H., Hussian, A.E.M., Abdel-Satar, A.M., Goher, M.E., Napiórkowska-Krzebietke, A. and Abd El-Monem, A.M., 2016. The isotherm and kinetic studies of the biosorption of heavy metals by non-living cells of chlorella vulgaris. *Journal of Elementology*, 21(4), pp.1263–1276.

Alkhatib, M.F., Muyibi, S.A. and Amode, J.O., 2011. Optimization of activated carbon production from empty fruit bunch fibers in one-step steam pyrolysis for cadmium removal from aqueous solution. *Environmentalist*, 31(4), pp.349–357.

Amini, M., Younesi, H. and Bahramifar, N., 2009. Biosorption of nickel(II) from aqueous solution by Aspergillus niger: Response surface methodology and isotherm study. *Chemosphere*, [online] 75(11), pp.1483–1491. Available at: <http://dx.doi.org/10.1016/j.chemosphere.2009.02.025>.

Aniyikaiye, T.E., Oluseyi, T., Odiyo, J.O. and Edokpayi, J.N., 2019. Physico-chemical analysis of wastewater discharge from selected paint industries in Lagos, Nigeria. *International Journal of Environmental Research and Public Health*, 16(7), pp.1–17.

Bagheri, R., Ghaedi, M., Asfaram, A., Alipanahpour Dil, E. and Javadian, H., 2019. RSM-CCD design of malachite green adsorption onto activated carbon with multimodal pore size distribution prepared from Amygdalus scoparia: Kinetic and isotherm studies. *Polyhedron*, [online] 171, pp.464–472. Available at: <https://doi.org/10.1016/j.poly.2019.07.037>.

Bahadir, T., Bakan, G., Altas, L. and Buyukgungor, H., 2007. The investigation of lead removal by biosorption: An application at storage battery industry wastewaters. *Enzyme and Microbial Technology*, 41(1–2), pp.98–102.

Benjamin, M.M. and Lawler, D.F., 2013. Part IV: Membrane-Based Water and Wastewater Treatment. In: *Water Quality Engineering: Physical / Chemical Treatment Processes*. John Wiley & Sons, Inc., pp.731–838.

Bhatnagar, A. and Minocha, A.K., 2010. Biosorption optimization of nickel removal from water using Punica granatum peel waste. *Colloids and Surfaces B: Biointerfaces*, 76(2), pp.544–548.

Biswas, S., Bal, M., Behera, S.K., Sen, T.K. and Meikap, B.C., 2019. Process optimization study of Zn 2+ adsorption on biochar-alginate composite adsorbent by response surface methodology (RSM). *Water (Switzerland)*, 11(2), pp.1–15.

Bouhamed, F., Elouear, Z., Bouzid, J. and Ouddane, B., 2014. Batch sorption of Pb(II) ions from aqueous solutions using activated carbon prepared from date stones: Equilibrium, kinetic, and thermodynamic studies. *Desalination and Water Treatment*, 52(10–12), pp.2261–2271.

Bulut, Y. and Tez, Z., 2007. Adsorption studies on ground shells of hazelnut and almond. *Journal of Hazardous Materials*, [online] 149(1), pp.35–41. Available at: <http://www.sciencedirect.com/science/article/pii/S0304389407004104>.

Bushra, R., Ahmed, A. and Shahadat, M., 2017. *CHAPTER 5: Mechanism of Adsorption on Nanomaterials*. [online] *RSC Detection Science*, Elsevier Inc. Available at: <http://dx.doi.org/10.1016/B978-0-12-812792-6/00004-2>.

Butani, S.A. and Mane, S.J., 2017. Coagulation/Flocculation Process for Cationic, Anionic Dye Removal Using Water Treatment Residuals – a Review. *International Journal of Science Technology and Management*, [online] 6(4), pp.1–5. Available at: <https://pdfs.semanticscholar.org/af27/5e4c97b2ac4c9da1c0812b25938521cb1613.pdf>.

Cempel, M. and Nikel, G., 2006. Nickel: A Review of Its Sources and Environmental Toxicology. *Polish Journal of Environmental Studies*, [online] 15(3), pp.375–382. Available at: <http://www.nickeltest.net/download/375-382.pdf>.

Ceyhan, A.A., Şahin, Ö., Saka, C. and Yalçin, A., 2013. A novel thermal process for activated carbon production from the vetch biomass with air at low temperature by two-stage procedure. *Journal of Analytical and Applied Pyrolysis*, 104(March 2018), pp.170–175.

Chen, C.Y. and Lin, T.H., 1998. Nickel toxicity to human term placenta: In vitro study on lipid peroxidation. *Journal of Toxicology and Environmental Health - Part A*, 54(1), pp.37–47.

Chen, J.P., Yang, L., Ng, W.-J., Wang, L.K. and Thong, S.-L., 2006. Ion Exchange. In: L.K. Wang, Y.-T. Hung and N.K. Shammas, eds., *Advanced Physicochemical Treatment Processes*, 4th ed. Totowa, NJ: The Humana Press Inc.

Chowdhury, Z.Z., Krishnan, B., Sagadevan, S., Rafique, R.F., Hamizi, N.A.B., Wahab, Y.A., Khan, A.A., Bin Johan, R., Al-Douri, Y., Kazi, S.N. and Shah, S.T., 2018. Effect of temperature on the physical, electro-chemical and adsorption properties of carbon micro-spheres using hydrothermal carbonization process. *Nanomaterials*, 8(8), pp.1–19.

Christoforidis, A.K., Orfanidis, S., Papageorgiou, S.K., Lazaridou, A.N., Favvas, E.P. and Mitropoulos, A.C., 2015. Study of Cu(II) removal by Cystoseira crinitophylla biomass in batch and continuous flow biosorption. *Chemical Engineering Journal*, [online] 277, pp.334–340. Available at: <http://dx.doi.org/10.1016/j.cej.2015.04.138>.

Cobzaru, C. and Inglezakis, V., 2015. Chapter Ten - Ion Exchange. In: S.B.T.-P. in F. and S. Tarleton, ed., *Progress in Filtration and Separation*. [online] Oxford: Academic Press, pp.425–498. Available at: <http://www.sciencedirect.com/science/article/pii/B9780123847461000100>.

Crawford, C.B. and Quinn, B., 2017. 6 - The interactions of microplastics and chemical pollutants. In: C.B. Crawford and B.B.T.-M.P. Quinn, eds. [online] Elsevier, pp.131–157. Available at: <http://www.sciencedirect.com/science/article/pii/B9780128094068000062>.

Crist, R.H., Oberholser, K., Shank, N. and Nguyen, M., 1981. Nature of Bonding between Metallic Ions and Algal Cell Walls. *Environmental Science and Technology*, 15(10), pp.1212–1217.

Cuhadaroglu, D. and Uygun, O.A., 2008. Production and characterization of activated carbon from a bituminous coal by chemical activation. *African Journal of Biotechnology*, 7(20), pp.3706–3713.

Dantas, T.L.P., Amorim, S.M., Luna, F.M.T., Silva, I.J., de Azevedo, D.C.S., Rodrigues, A.E. and Moreira, R.F.P.M., 2010. Adsorption of carbon dioxide onto activated carbon and nitrogen-enriched activated carbon: Surface changes, equilibrium, and modeling of fixed-bed adsorption. *Separation Science and Technology*, 45(1), pp.73–84.

Davarnejad, R., Moraveji, M.K. and Havaie, M., 2018. Integral technique for evaluation and optimization of Ni (II) ions adsorption onto regenerated cellulose using response surface methodology. *Arabian Journal of Chemistry*, [online] 11(3), pp.370–379. Available at: <http://dx.doi.org/10.1016/j.arabjc.2015.05.022>.

Department of Environment, 2009. *Environmental Quality Act 1974. Department of Environment*. Available at: <https://www.doe.gov.my/portalv1/wp-content/uploads/2015/01/Environmental_Quality_Sewage_Regulations_2009_-_P.U.A_432-2009.pdf>.

Department of Environment, 2010. *Environmental Requirements: A Guide For Investors*. [online] *Ministry of Natural Resources and Environment*, Available at: <http://www.doe.gov.my/eia/wp-content/uploads/2012/03/A-Guide-For-Investors1.pdf>.

Dilek, F.B., Erbay, A. and Yetis, U., 2002. Ni(II) biosorption by Polyporous versicolor. *Process Biochemistry*, 37(7), pp.723–726.

Din, M.I. and Mirza, M.L., 2013. Biosorption potentials of a novel green biosorbent Saccharum bengalense containing cellulose as carbohydrate polymer for removal of Ni (II) ions from aqueous solutions. *International Journal of Biological Macromolecules*, [online] 54(1), pp.99–108. Available at: <http://dx.doi.org/10.1016/j.ijbiomac.2012.11.010>.

Duru, C.E. and Duru, I.A., 2017. Studies of Sorbent Efficiencies of Maize Parts in Fe(II) Removal from Aqueous Solutions. *International Letters of Chemistry, Physics and Astronomy*, 72(3), pp.1–8.

EMIS, 2010a. *Chemical Precipitation*. [online] Available at: <https://emis.vito.be/en/techniekfiche/chemical-precipitation> [Accessed 29 Jun. 2019].

EMIS, 2010b. *Coagulation and Flocculation*. [online] Available at: <https://emis.vito.be/nl/node/22515> [Accessed 30 Jun. 2019].

EMIS, 2019. *Ion-exchange*. [online] 2010. Available at: <https://emis.vito.be/en/techniekfiche/ion-exchange> [Accessed 29 Jun. 2019].

Flores-Garnica, J.G., Morales-Barrera, L., Pineda-Camacho, G. and Cristiani-Urbina, E., 2013. Biosorption of Ni(II) from aqueous solutions by Litchi chinensis seeds. *Bioresource Technology*, [online] 136, pp.635–643. Available at: <http://dx.doi.org/10.1016/j.biortech.2013.02.059>.

Foo, L.P.Y., Tee, C.Z., Raimy, N.R., Hassell, D.G. and Lee, L.Y., 2012. Potential Malaysia agricultural waste materials for the biosorption of cadmium(II) from aqueous solution. *Clean Technologies and Environmental Policy*, 14(2), pp.273–280.

Fu, F. and Wang, Q., 2011. Removal of heavy metal ions from wastewaters: a review. *Journal of environmental management*, [online] 92(3), pp.407–418. Available at: <http://www.ncbi.nlm.nih.gov/pubmed/21138785>.

Garba, Z.N., Ugbaga, N.I. and Abdullahi, A.K., 2016. Evaluation of optimum adsorption conditions for Ni (II) and Cd (II) removal from aqueous solution by modified plantain peels (MPP). *Beni-Suef University Journal of Basic and Applied Sciences*, [online] 5(2), pp.170–179. Available at:

<http://dx.doi.org/10.1016/j.bjbas.2016.03.001>.

Graff, M., 2012. 10 - Disposal of metalworking fluids. In: V.P. Astakhov and S.B.T.-M.F. (MWFs) for C. and G. Joksch, eds., *Woodhead Publishing Series in Metals and Surface Engineering*. [online] Woodhead Publishing, pp.389–402. Available at: <http://www.sciencedirect.com/science/article/pii/B9780857090614500104>.

Guo, X., Tang, S., Song, Y. and Nan, J., 2018. Adsorptive removal of Ni2+ and Cd2+ from wastewater using a green longan hull adsorbent. *Adsorption Science and Technology*, 36(1–2), pp.762–773.

Gupta, V.K., Rastogi, A. and Nayak, A., 2010. Biosorption of nickel onto treated alga (Oedogonium hatei): Application of isotherm and kinetic models. *Journal of Colloid and Interface Science*, [online] 342(2), pp.533–539. Available at: <http://dx.doi.org/10.1016/j.jcis.2009.10.074>.

Gürel, L., 2017. Applications of the biosorption process for nickel removal from aqueous solutions - a review. *Chemical Engineering Communications*, 204(6), pp.711–722.

Home Water Purification Systems, 2019. *Ion Exchange (Water Softeners)*. [online] Available at: <https://sites.google.com/a/cherrycreekschools.org/water-treatment-systems/home-water-treatment-systems/ion-exchange-water-softeners> [Accessed 20 Aug. 2019].

Huang, M.R., Li, S. and Li, X.G., 2010. Longan shell as novel biomacromolecular sorbent for highly selective removal of lead and mercury ions. *Journal of Physical Chemistry B*, 114(10), pp.3534–3542.

Hung, Y.-T., Lo, H.H., Wang, L.K., Taricska, J.R. and Li, K.H., 2006. Powdered Activated Carbon Adsorption. In: and N.K.S. L. K. Wang, Y.-T. Hung, ed., *Advanced Physicochemical Treatment Processes*, 4th ed. Totowa, NJ: The Humana Press Inc.

Husain, A., Javed, I., Khan, N.A., Section, C.E., Engg, F.O. and Aligarh, U.P., 2014. Characterization and treatment of electroplating industry wastewater using Fenton's reagent. *Journal of Chemical and Pharmaceutical Research*, 6(1), pp.622–627.

Jafarinejad, S., 2017. 6 - Treatment of Oily Wastewater. In: S.B.T.-P.W.T. and P.C. Jafarinejad, ed. [online] Butterworth-Heinemann, pp.185–267. Available at: <http://www.sciencedirect.com/science/article/pii/B9780128092439000067>.

Javanbakht, V. and Ghoreishi, S.M., 2017. Application of response surface methodology for optimization of lead removal from an aqueous solution by a novel superparamagnetic nanocomposite. *Adsorption Science and Technology*, 35(1–2), pp.241–260.

Joglekar, A.M. and May, A.T., 1987. Product Excellence through Design of Experiments. *Cereal Foods World*, 32, pp.857–868.

Joseph, L., 2013. *Drinking water quality assessment and application of nanotechnology and electrochemical techniques in water treatment*. [online] Kannur University. Available at: <https://shodhganga.inflibnet.ac.in/bitstream/10603/84539/13/13.chapter7.pdf>.

Kabdaşli, I., Arslan, T., Ölmez-Hanci, T., Arslan-Alaton, I. and Tünay, O., 2009. Complexing agent and heavy metal removals from metal plating effluent by electrocoagulation with stainless steel electrodes. *Journal of Hazardous Materials*, 165(1–3), pp.838–845.

Kalyani, S., Srinivasa Rao, P. and Krishnaiah, A., 2004. Removal of nickel (II) from aqueous solutions using marine macroalgae as the sorbing biomass. *Chemosphere*, 57(9), pp.1225–1229.

Kanamarlapudi, S.L.R.K., Chintalpudi, V.K. and Muddada, S., 2018. Application of Biosorption for Removal of Heavy Metals from Wastewater. In: J. Derco and B. Vrana, eds., *Biosorption*, 1st ed. [online] Guntur: IntechOpen, pp.69–115. Available at: <https://doi.org/10.5772/intechopen.77315>.

Keçili, R. and Hussain, C.M., 2018. Mechanism of Adsorption on Nanomaterials. In: *Nanomaterials in Chromatography*. pp.89–115.

Kowanga, K.D., Gatebe, E., Mauti, G.O. and Mauti, E.M., 2016. Kinetic , sorption isotherms , pseudo-first-order model and pseudo-second-order model studies of Cu (II) and Pb (II) using defatted Moringa oleifera seed powder. *The journal of phytopharmacology*, [online] 5(2), pp.71–78. Available at: <www.phytopharmajournal.com>.

Kulkarni, R.M., Shetty, K.V. and Srinikethan, G., 2014. Cadmium (II) and nickel (II) biosorption by Bacillus laterosporus (MTCC 1628). *Journal of the Taiwan Institute of Chemical Engineers*, [online] 45(4), pp.1628–1635. Available at: <http://dx.doi.org/10.1016/j.jtice.2013.11.006>.

Kurniawati, D., Lestari, I., Sy, S., Harmiwati, Aziz, H., Chaidir, Z. and Zein, R., 2016. Removal of Cu(II) from aqueous solutions using shell and seed of Kelengkengfruits (Euphoria longan Lour). *Der Pharma Chemica*, 8(14), pp.149–154.

Li, S. and Tao, M., 2016. Removal of cationic dyes from aqueous solutions by a low-cost biosorbent: longan shell. *Desalination and Water Treatment*, 57(11), pp.5193–5199.

Lin, M.G., Lasekan, O., Saari, N. and Khairunniza-Bejo, S., 2018. Effect of chitosan and carrageenan-based edible coatings on post-harvested longan (Dimocarpus longan) fruits . *CyTA - Journal of Food*, 16(1), pp.490–497.

Liu, H., Shi, A., Liu, L., Wu, H., Ma, T., He, X., Lin, W., Feng, X. and Liu, Y., 2016. *Peanut Protein Processing Technology*. 1st ed. *Peanuts: Processing Technology and Product Development*. Beijing.

Liu, L., Luo, X.-B., Ding, L. and Luo, S.-L., 2019. *Application of Nanotechnology in the Removal of Heavy Metal From Water*. 1st ed. [online] *Nanomaterials for the Removal of Pollutants and Resource Reutilization*. Wuhan: Elsevier Inc. Available at: <http://dx.doi.org/10.1016/B978-0-12-814837-2.00004-4>.

Lorza, R.L., Calvo, M.Á.M., Labari, C.B. and Fuente, P.J.R., 2018. Using the multi-response method with desirability functions to optimize the Zinc electroplating of steel screws. *Metals*, 8(9), pp.1–20.

Mazille, F. and Spuhler, D., 2019. *Adsorption (Activated Carbon)*. [online] SSWM. Available at: <https://sswm.info/sswm-university-course/module-6-disaster-situations-planning-and-preparedness/further-resources-0/adsorption-%28activated-carbon%29> [Accessed 1 Jul. 2019].

Mazille, F. and Spuhler, D., 2019. *Membrane Filtration*. [online] SSWM University Course. Available at: <https://sswm.info/sswm-university-course/module-6-disaster-situations-planning-and-preparedness/further-resources-0/membrane-filtration> [Accessed 29 Jun. 2019].

Mohammed, A.A., Najim, A.A., Al-Musawi, T.J. and Alwared, A.I., 2019. Adsorptive performance of a mixture of three nonliving algae classes for nickel remediation in synthesized wastewater. *Journal of Environmental Health Science and Engineering*, 17(2), pp.529–538.

Montazer-Rahmati, M.M., Rabbani, P., Abdolali, A. and Keshtkar, A.R., 2011. Kinetics and equilibrium studies on biosorption of cadmium, lead, and nickel ions from aqueous solutions by intact and chemically modified brown algae. *Journal of Hazardous Materials*, [online] 185(1), pp.401–407. Available at: <http://dx.doi.org/10.1016/j.jhazmat.2010.09.047>.

Moyo, M., Nyamhere, G., Sebata, E. and Guyo, U., 2016. Kinetic and equilibrium modelling of lead sorption from aqueous solution by activated carbon from goat dung. *Desalination and Water Treatment*, 57(2), pp.765–775.

National Programme on Technology Enhanced Learning (NPTEL), 2019. *Electrochemical Treatment*. [online] Available at: <https://nptel.ac.in/courses/103107084/module3/lecture14/lecture14.pdf> [Accessed 30 Jun. 2019].

Oghenejoboh, K.M., 2018. Biosorption of nickel (II) ion from synthetic wastewater on watermelon rind activated carbon using reponse surface methodology (RSM) optimization approach. *Nigerian Journal of Technology*, 37(3), pp.647–655.

Ouyang, D., Zhuo, Y., Hu, L., Zeng, Q., Hu, Y. and He, Z., 2019. Research on the adsorption behavior of heavy metal ions by porous material prepared with silicate tailings. *Minerals*, 9(5), pp.1–16.

Özer, A., Özer, D. and Ekiz, H.I., 2005. The equilibrium and kinetic modelling of the biosorption of copper(II) ions on cladophora crispata. *Adsorption*, 10(4), pp.317–326.

Ozsoy, H.D. and van Leeuwen, J. (Hans), 2012. Fungal Biosorption of Ni (II) Ions. *Green Energy and Technology*, 62, pp.45–58.

Öztürk, A., Artan, T. and Ayar, A., 2004. Biosorption of nickel(II) and copper(II) ions from aqueous solution by Streptomyces coelicolor A3(2). *Colloids and Surfaces B: Biointerfaces*, 34(2), pp.105–111.

Ozturk, D., Şahan, T., Bayram, T. and Erkuş, A., 2017. Application of Response Surface Methodology (RSM) to optimize the adsorption conditions of Cationic Basic Yellow 2 onto pumice samples as a new adsorbent. *Fresenius Environmental Bulletin*, 26, pp.3285–3292.

Padmavathy, V., 2008. Biosorption of nickel(II) ions by baker's yeast: Kinetic, thermodynamic and desorption studies. *Bioresource Technology*, 99(8), pp.3100–3109.

Pahlavanzadeh, H., Keshtkar, A.R., Safdari, J. and Abadi, Z., 2010. Biosorption of nickel(II) from aqueous solution by brown algae: Equilibrium, dynamic and thermodynamic studies. *Journal of Hazardous Materials*, 175(1–3), pp.304–310.

Palmer, K., Ronkanen, A.K. and Kløve, B., 2015. Efficient removal of arsenic, antimony and nickel from mine wastewaters in Northern treatment peatlands and potential risks in their long-term use. *Ecological Engineering*, [online] 75, pp.350–364. Available at: <http://dx.doi.org/10.1016/j.ecoleng.2014.11.045>.

Papageorgiou, S.K., Katsaros, F.K., Kouvelos, E.P. and Kanellopoulos, N.K., 2009. Prediction of binary adsorption isotherms of Cu2+, Cd2+ and Pb2+ on calcium alginate beads from single adsorption data. *Journal of Hazardous Materials*, 162(2–3), pp.1347–1354.

Papirio, S., Frunzo, L., Mattei, M.R., Ferraro, A., Race, M., D'Acunto, B., Pirozzi, F. and Esposito, G., 2017. Heavy Metal Removal from Wastewaters by Biosorption: Mechanisms and Modeling. In: E.R. Rene, E. Sahinkaya, A. Lewis and P.N.L. Lens, eds., *Sustainable Heavy Metal Remediation: Volume 1: Principles and Processes*. [online] Cham: Springer International Publishing, pp.25–63. Available at: <https://doi.org/10.1007/978-3-319-58622-9_2>.

Park, D., Yun, Y.S. and Park, J.M., 2010. The past, present, and future trends of biosorption. *Biotechnology and Bioprocess Engineering*, 15(1), pp.86–102.

Pathak, P.D., Mandavgane, S.A. and Kulkarni, B.D., 2017. Fruit peel waste: Characterization and its potential uses. *Current Science*, 113(3), pp.444–454.

Pelegri, A.A. and Tekkam, A., 2003. Optimization of laminates' fracture toughness using design of experiments and response surface. *Journal of Composite Materials*, 37(7), pp.579–596.

Popuri, S.R., Vijaya, Y., Boddu, V.M. and Abburi, K., 2009. Adsorptive removal of copper and nickel ions from water using chitosan coated PVC beads. *Bioresource Technology*, 100(1), pp.194–199.

Porex Corporation, 2013. *POREX ® Tubular Membrane Filter (TMF^{TM}) Applied in Copper / Nickel Wastewater Treatment System for an Electroplating Industry Park.* [online] Available at: <http://www.porexfiltration.com/files/documents/Case-Study---TMF-in-Electroplating-Park-for-CopperNickel-WastewaterTreatment-(3).pdf> [Accessed 8 Jan. 2020].

Rangkadilok, N., Sitthimonchai, S., Worasuttayangkurn, L., Mahidol, C., Ruchirawat, M. and Satayavivad, J., 2007. Evaluation of free radical scavenging and antityrosinase activities of standardized longan fruit extract. *Food and Chemical Toxicology*, 45(2), pp.328–336.

Rashed, M.N., 2013. Adsorption Technique for the Removal of Organic Pollutants from Water and Wastewater. In: M.N. Rashed, ed., *Organic Pollutants - Monitoring, Risk and Treatment*, 1st ed. [online] Rijeka: IntechOpen. Available at: <https://doi.org/10.5772/54048>.

Royal Society of Chemistry, 2019. *Periodic Table: Nickel*. [online] Available at: <http://www.rsc.org/periodic-table/element/28/nickel> [Accessed 20 Aug. 2019].

Ruckelshaus, W.D., Ravan, J.E. and Johnson, E., 1984. *Development Document for Effluent Limitations Guidelines and Standards for the Battery Manufacturing Point Source Category*. Washington, D.C.

Sadhukhan, B., Mondal, N.K. and Chattoraj, S., 2016. Optimisation using central composite design (CCD) and the desirability function for sorption of methylene blue from aqueous solution onto Lemna major. *Karbala International Journal of Modern Science*, [online] 2(3), pp.145–155. Available at: <http://www.sciencedirect.com/science/article/pii/S2405609X15301408>.

Sahu, O., Rao, D.G., Gopal, R., Tiwari, A. and Pal, D., 2017. Treatment of wastewater from sugarcane process industry by electrochemical and chemical process: Aluminum (metal and salt). *Journal of Water Process Engineering*, [online] 17, pp.50–62. Available at: <http://dx.doi.org/10.1016/j.jwpe.2017.03.005>.

Sahu, O. and Singh, N., 2019. Significance of bioadsorption process on textile industry wastewater. In: B.S. Butola and Shahid-ul-Islam, eds., *The Impact and Prospects of Green Chemistry for Textile Technology*, 1st ed. [online] Delhi: Elsevier Ltd., pp.367–416. Available at: <https://doi.org/10.1016/B978-0-08-102491-1.00013-7>.

Saravanan, A., Senthil Kumar, P. and Preetha, B., 2016. Optimization of process parameters for the removal of chromium(VI) and nickel(II) from aqueous solutions by mixed biosorbents (custard apple seeds and Aspergillus niger) using response surface methodology. *Desalination and Water Treatment*, 57(31), pp.14530–14543.

Savolainen, H., 1996. Biochemical and clinical aspects of nickel toxicity. *Reviews on Environmental Health*, 11(4), pp.167–173.

Schweitzer, L. and Noblet, J., 2017. Water Contamination and Pollution. In: B. Török and T. Dransfield, eds., *Green Chemistry: An Inclusive Approach*, 1st ed.

Boston: Elsevier, pp.261–290.

Selatnia, A., Madani, A., Bakhti, M.Z., Kertous, L., Mansouri, Y. and Yous, R., 2004. Biosorption of Ni2+ from aqueous solution by a NaOH-treated bacterial dead Streptomyces rimosus biomass. *Minerals Engineering*, 17(7–8), pp.903–911.

Shih, Y., Lin, C. and Huang, Y., 2013. Application of Fered-Fenton and chemical precipitation process for the treatment of electroless nickel plating wastewater. *Separation and Purification Technology*, [online] 104, pp.100–105. Available at: <http://dx.doi.org/10.1016/j.seppur.2012.11.025>.

Shimadzu Corporation, 2020. *FTIR Analysis Q&A*. [online] Available at: <https://www.shimadzu.com/an/ftir/support/faq/4.html> [Accessed 17 Apr. 2020].

Shukla, A., Zhang, Y.-H., Dubey, P., Margrave, J.L. and Shukla, S.S., 2002. The role of sawdust in the removal of unwanted materials from water. *Journal of Hazardous Materials B95*, pp.137–152.

Singh, M. and Verghese, S., 2006. Physico-Chemical Investigation of Waste Water from Electroplating Industry at Agra and Technologies for Metal Removal and Recovery of Water. *National Seminar on Rainwater Harvesting and Water Management*, pp.397–401.

Singh, V. and Ram, C., 2016. Physico-Chemical Characterization of Electroplating Industrial Effluents of Chandigarh and Haryana Region. *Journal of Civil & Environmental Engineering*, 6(4), pp.1–6.

Sivakumar, D., Nouri, J., Modhini, T.M. and Deepalakshmi, K., 2018. Nickel removal from electroplating industry wastewater : A bamboo activated carbon. *Global. J. Environ. Sci. Manage.*, [online] 4(3), pp.325–338. Available at: <http://www.gjesm.net/article_31501.html>.

Sohbatzadeh, H., Keshtkar, A.R., Safdari, J. and Fatemi, F., 2016. U(VI) biosorption by bi-functionalized Pseudomonas putida @ chitosan bead: Modeling and optimization using RSM. *International Journal of Biological Macromolecules*, [online] 89, pp.647–658. Available at: <http://www.sciencedirect.com/science/article/pii/S0141813016304251>.

Srisuwan, G. and Thongchai, P., 2002. Removal of heavy metals from electroplating wastewater by membrane. *Membrane Sci & Tech*, 24(3), pp.965–976.

Srivastava, S., Agrawal, S.B. and Mondal, M.K., 2015. Biosorption isotherms and kinetics on removal of Cr(VI) using native and chemically modified Lagerstroemia speciosa bark. *Ecological Engineering*, [online] 85, pp.56–66. Available at: <http://dx.doi.org/10.1016/j.ecoleng.2015.10.011>.

Stat-Ease Inc., 2020. *Diagnostics Plots*. [online] Available at: <https://www.statease.com/docs/v11/contents/analysis/diagnostics/diagnostics-plots/> [Accessed 14 Apr. 2020].

Stat-Ease Inc., 2020. *Response Surface (pt 2)*. [online] Available at: <https://www.statease.com/docs/v11/tutorials/multifactor-rsm-pt2/> [Accessed 19 Apr. 2020].

Subbareddy, Y., 2015. *Equilibrium kinetics and thermodynamics of the adsorption of textile dyes Safranin O Rhodamine B Malachite Green Acid blue 113 and Acid blue 9 on Fullers Earth modified Fullers Earth and the activated carbon derived from Peltophorum pterocarpum leaves*. [online] The Shodhganga@INFLIBNET Centre. Available at: <https://shodhganga.inflibnet.ac.in/bitstream/10603/195223/3/chapter 1.pdf> [Accessed 25 Aug. 2019].

Tang, Y.Y., He, X.M., Sun, J., Li, C.B., Li, L., Sheng, J.F., Xin, M., Li, Z.C., Zheng, F.J., Liu, G.M., Li, J.M. and Ling, D.N., 2019. Polyphenols and alkaloids in byproducts of longan fruits (Dimocarpus longan Lour.) and their bioactivities. *Molecules*, 24(6), pp.1–16.

Teh, C.Y., Budiman, P.M., Shak, K.P.Y. and Wu, T.Y., 2016. Recent Advancement of Coagulation-Flocculation and Its Application in Wastewater Treatment. *Industrial and Engineering Chemistry Research*, 55(16), pp.4363–4389.

Tolian, G., Jafari, S.A. and Zarei, S., 2015. Optimization of biosorption of nickel(II) and cadmium(II) by indigenous seaweed enteromorpha using response surface methodology. *Water Quality Research Journal of Canada*, 50(2), pp.109–122.

Tseng, H., Wu, W., Huang, H. and Wu, M., 2013. Quantification of Fractions from Longan Seeds and Their Antimicrobial Activity. *International Journal of Medical Sciences and Biotechnology*, 1(4), pp.9–17.

Vieira, M.G.A., Neto, A.F.A., Gimenes, M.L. and da Silva, M.G.C., 2010. Sorption kinetics and equilibrium for the removal of nickel ions from aqueous phase on calcined Bofe bentonite clay. *Journal of Hazardous Materials*, [online] 177(1–3), pp.362–371. Available at: <http://dx.doi.org/10.1016/j.jhazmat.2009.12.040>.

Wang, F., Lu, X. and Li, X.Y., 2016. Selective removals of heavy metals (Pb2+, Cu2+, and Cd2+) from wastewater by gelation with alginate for effective metal recovery. *Journal of Hazardous Materials*, [online] 308, pp.75–83. Available at: <http://dx.doi.org/10.1016/j.jhazmat.2016.01.021>.

Wang, L.K., Vaccari, D.A., Li, Y. and Shammas, N.K., 2005. Chemical Precipitation. In: L.K. Wang, Y.-T. Hung and N.K. Shammas, eds., *Physicochemical Treatment Processes*. [online] Totowa, NJ: Humana Press, pp.141–197. Available at: <https://doi.org/10.1385/1-59259-820-x:141>.

Wang, Y., Zhu, L., Jiang, H., Hu, F. and Shen, X., 2016. Application of longan shell as non-conventional low-cost adsorbent for the removal of cationic dye from aqueous solution. *Spectrochimica Acta - Part A: Molecular and Biomolecular Spectroscopy*, [online] 159, pp.254–261. Available at: <http://dx.doi.org/10.1016/j.saa.2016.01.042>.

Water Environment Partnership in Asia, 2006. *National Water Quality Standards For Malaysia*. [online] Available at: <http://wepa-db.net/3rd/en/topic/waterstandard/Malaysia_1_surface.pdf> [Accessed 21 Aug. 2019].

World Health Organization, 2005. *Nickel in Drinking-water*. [online] Available at: <https://www.who.int/water_sanitation_health/gdwqrevision/nickel2005.pdf> [Accessed 12 Jun. 2019].

Xu, F., Yu, J., Tesso, T., Dowell, F. and Wang, D., 2013. Qualitative and quantitative analysis of lignocellulosic biomass using infrared techniques: A mini-review. *Applied Energy*, [online] 104, pp.801–809. Available at: <http://dx.doi.org/10.1016/j.apenergy.2012.12.019>.

Yadav, M., Gupta, R. and Sharma, R.K., 2019. Chapter 14 - Green and Sustainable Pathways for Wastewater Purification. In: S.B.T.-A. in W.P.T. Ahuja, ed., *Advances in Water Purification Techniques: Meeting the Needs of Developed and Developing Countries*. [online] Elsevier, pp.355–383. Available at: <http://www.sciencedirect.com/science/article/pii/B9780128147900000144>.

Zafar, M.N., Nadeem, R. and Hanif, M.A., 2007. Biosorption of nickel from protonated rice bran. *Journal of Hazardous Materials*, [online] 143(1), pp.478–485. Available at: <http://www.sciencedirect.com/science/article/pii/S0304389406011241>.